2017

THE INFLUENCE OF TREE HEIGHT ON LIDAR'S ABILITY TO ACCURATELY CHARACTERIZE FOREST STRUCTURE AND SPATIAL PATTERN ACROSS REFERENCE LANDSCAPES

Haley L. Wiggins
The University Of Montana

THE INFLUENCE OF TREE HEIGHT ON LIDAR'S ABILITY TO ACCURATELY CHARACTERIZE FOREST STRUCTURE AND SPATIAL PATTERN ACROSS REFERENCE LANDSCAPES

By

HALEY LANING WIGGINS

B.S. University of Montana, Missoula, Montana 2009

Thesis

presented in partial fulfillment of the requirements
for the degree of

Master of Science
in Resource Conservation

The University of Montana
Missoula, MT

May 2017

Approved by:

Scott Whittenburg, Dean of The Graduate School
Graduate School

Dr. Cara Nelson
Department of Ecosystem Sciences

Dr. Andrew Larson
Department of Forest Management

Dr. Jon Graham
Department of Mathematical Sciences

Wiggins, Haley, Master of Science, May 2017 Resource Conservation

Abstract

Committee Chair: Dr. Cara Nelson

Successful restoration of degraded forest landscapes requires reference models that adequately capture structural heterogeneity at multiple spatial scales. Field-based methods for assessing variation in forest structure are costly and inherently suffer from limited replication and spatial coverage. LiDAR is a more cost-effective approach for generating landscape-scale data, but it has a limited ability to detect understory trees. Increased understanding of appropriate height cut-offs for trees to be reliably included in LiDAR-based analysis could improve applications of LiDAR to assessments of landscape-scale forest structure. Toward that end, I investigated the effect of varying tree-height criterion (minimum height cutoffs of 6, 9, 12, 15, and 18 m) on the accuracy of LiDAR for estimating forest structure and spatial pattern in forests of the Sierra de San Pedro Martir National Park, Baja, Mexico. In order to increase the utility of the analysis, LiDAR trees were identified using a widely-available processing tool (FUSION's TreeSeg). Accuracy was measured as the similarity between field-measured and LiDAR-detected tree datasets and was assessed for overall number of trees, spatial tree density maps, and a set of variables related to forest structure and spatial pattern. I found that removing trees less than 12 m in height increased correlation between LiDAR- and field-based spatial maps of tree density and strongly reduced differences in estimates of forest structure and spatial pattern. Although the frequency of small, medium, and large tree clumps was always underestimated by LiDAR-detected trees, the 12 m minimum height cutoff detected more of the large tree clumps than taller height cutoffs and provided estimates of forest structure and spatial pattern that were more similar to those derived from field data. The 12 m height cutoff also successfully captured structural variation across the study landscape: canyons, shallow northerly, and shallow southerly slopes were structurally similar, having larger and more abundant trees than steep northerly slopes, steep southerly slopes, and ridges. Methods developed here should be useful to managers interested in using LiDAR to characterize distributions of large, overstory trees without the need for extensive complementary field data and specifically for the development of landscape-scale reference models for forest management and restoration.

Introduction

Across the globe, forest management is increasingly focusing on restoration of highly degraded, ecologically vulnerable forest types (Schoennagel and Nelson 2011). Successful forest restoration requires reference models that adequately capture structural heterogeneity at multiple spatial scales (Hessburg et al. 2015, Larson and Churchill 2012). Although current management recommendations call for planning and implementing restoration activities at the landscape scale (North et al. 2009, 2012), there is a lack of information on best practices for reference model development at that scale. LiDAR (light detection and ranging) allows for high-resolution characterization of forest structure over extensive areas (Stephens et al. 2015, Kane et al. 2013); however, directly translating complex LiDAR data into management-relevant descriptions of forest structure (i.e. size distributions and arrangements of individual trees and tree clumps) is challenging. A primary limitation is that LiDAR does not reliably capture understory trees (Falkowski et al. 2008, Kaartinen et al. 2012). Although it is well known that tall trees have higher detection rates than short trees (Richardson and Moskal 2011), there is little information about appropriate minimum height cutoffs for generating accurate structural estimates of taller trees. In this study, I assess how varying the minimum tree height cutoff affects the accuracy of LiDAR for characterizing forest structure in the Sierra de San Pedro Martir National Park, Baja, Mexico and determine whether the application of the relevant tree-height cutoff captures structural variation across an extensive, relatively undisturbed forested landscape.

Successful restoration depends on ecological reference models, which approximate the set of conditions an ecosystem would be in if it had never been altered or degraded (McDonald et al. 2016). Creating reference models for forest restoration requires a large number of replicates within and among stands in order to capture inherent variability (SER 2016, Swetnam et al. 1999). Although recent field-based studies of reference conditions have included within-stand (e.g. Lydersen et al. 2013) or among stand (e.g. Sanchez Maedor et al. 2011, Abella and Denton 2009, Churchill et al. 2015) replication, none have used both types of replication and all are based on relatively small sample areas (1-4 ha plot sizes) with limited total spatial coverage (maximum = 52 ha (Abella and Denton 2009)). One reason for the lack of replication is that investigators rely on field-measured stem maps to capture fine-scale heterogeneity (Larson and Churchill 2012). Although field-measured stem maps provide precise location data for all individual trees, they are expensive to sample. LiDAR, when used with Individual tree detection (ITD) processes, is 2 - 3 orders of magnitude less expensive than field-measured stem maps (Jeronimo 2015). ITD methods, however, fail to detect overtopped (understory) trees and, therefore, the performance of ITD varies among forest types based on stand density, structural complexity and dominant tree height (Vauhkonen et al. 2012, Li et al. 2012, Kaartinen et al. 2012, Falkowski et al. 2008). There are other methods of structural analysis using LiDAR, such as area-based methods, which quantify forest structure within discrete units that usually represent field plots or raster cells (Richardson and Moslak 2012). Area-based methods, however, often require costly and time-consuming complementary field data, are incapable of capturing fine-scale heterogeneity (i.e. the distribution of single trees), and have lower accuracy than ITD approaches (Richardson and Moslak 2012, Breidenbach 2010, Kaartinen et al. 2012).

Identification of the locations of individual trees is critical for assessing forest spatial pattern (i.e. the arrangement of individual trees relative to one another). In the past, reference models for restoration

have included composition and structure but not spatial pattern, but today there is increasing recognition of the importance of including spatial pattern in these models, due to emerging ideas about links between pattern and ecosystem process (e.g. Churchill et al. 2015, Sanchez Maedor et al. 2011, Abella and Denton 2009, Lydersen et al. 2013, Fry et al. 2014). Intact forests exhibit structural heterogeneity across multiple spatial scales; this heterogeneity depends upon pattern and process feedbacks, in which climate and disturbance effects are both reflected in and affected by current forest conditions (Larson and Churchill 2012, North et al. 2009, Hessburg et al. 2015). For example, the spacing of trees and canopy openings in fire-adapted forests reflects resource availability and the local historic fire regime; in turn, patterns of trees and canopy openings affect resilience to future wildfires and pest outbreaks, as well as water and carbon cycling rates and the population dynamics of dominant tree species (Kane et al. 2015, Larson and Churchill 2012, North et al. 2009, 2012, Lydersen et al. 2014, Sanchez Maedor et al. 2011).

Because overstory spatial pattern varies among forest stands across landscapes, it is necessary to describe pattern across the range of forest stands within a landscape (North et al. 2009). As aspect and slope position change, so do significant controls on forest structure, including substrate characteristics (e.g. soil depth, drainage, and erosion rates), disturbance histories (e.g. fire severity, time since last fire), and climatic water balance (e.g. actual evapotranspiration, water deficit) (Dobrowski 2011, Meyer et al. 2007b, Milodowski et al. 2014, Kane et al. 2013). Numerous studies relating forest structure to local physiography have been published to date (e.g. Taylor and Skinner 2003, Hessburg et al. 2007, Underwood et al. 2010, Lydersen and North 2012, Kane et al. 2015); however, variation in forest structure and spatial pattern across an extensive, modern reference landscape has not been quantified. Understanding how forest structure and spatial pattern varies across reference landscapes will allow managers to tailor restoration treatments to specific landforms within their project areas (North et al. 2009, 2012).

Managers and scientists alike acknowledge the need for structural reference models to inform restoration activities in degraded, fire-dependent landscapes of western North America (North et al. 2009, 2012, Hessburg et al. 2015, Franklin and Johnson 2012). Limited spatial coverage precludes the ability of field data to capture landscape-scale structural variation, and LiDAR area-based methods fail to describe fine-scale heterogeneity; LiDAR ITD approaches have the greatest potential to characterize structural variation at multiple spatial scales in management-relevant terms. While mid- and under-story trees are the primary source of ITD errors, reported detection rates for dominant trees are very high for a range of forest conditions (Vauhkonen et al. 2012, Kaartinen et al. 2012, Falkowski et al. 2008). Richardson and Moskal (2011) produced accurate, unbiased density estimates of trees greater than 20 m tall using ITD. These studies suggest that excluding trees below a specific height could significantly improve ITD-based characterizations of overstory structure and spatial pattern, and highlight the need to formally investigate the effect of minimum height cutoffs on the accuracy of structure and spatial pattern estimates. In order to maximize the accessibility of the approach, I used FUSION's TreeSeg tool to detect individual trees; FUSION is a free, commonly-used, and widely-available software package for LiDAR processing developed by the USDA Forest Service. My specific research objectives were to:

1) Determine a recommended minimum tree height cutoff for using TreeSeg to describe forest structure over extensive areas by removing incrementally taller trees from comparisons of

LiDAR-detected and field-measured tree distributions. Specifically, I assessed how varying the minimum tree height cutoff affects the accuracy of LiDAR (using FUSION's TreeSeg tool) to characterize number of trees; spatial tree density maps (at three resolutions); and estimates of forest structure and spatial pattern.

2) Test the ability of LiDAR-detected trees above the recommended minimum height cutoff to capture structural variation across forested landscapes in order to build reliable, large-scale reference models. Specifically, I quantified structure and spatial pattern using LiDAR trees above the recommended height cutoff within six distinct landforms (canyons, ridges, steep and shallow northerly slopes, and steep and shallow southerly slopes) and tested for statistical differences using multivariate and univariate analyses.

Methods

Study Area

This study was conducted in the Parque Nacional Sierra de San Pedro Martir (SSPM) of Baja, Mexico (Fig. 1), which is considered to be the most extensive remaining reference area for fire-adapted dry forests of western North America (Fry et al. 2014, Dunbar-Irwin and Safford 2016). Limited logging has occurred and although fire suppression began in the mid-1970s, this landscape has yet to exhibit the structural changes evident in most other frequent-fire forests of North America, probably because tree growth and mortality rates are low (Dunbar-Irwin and Safford 2016, Stephens and Fry 2008). In particular, the park has been proposed as a suitable reference area for forests of the eastern Sierra Nevada because of their high degree of similarity (Minnich et al. 2000, Stephens and Fule 2005, Dunbar-Irwin and Safford 2016). In the SSPM, Jeffrey pine (*Pinus jeffreyi*) is the dominant conifer and occurs in monocultures and with white fir (*Abies concolor*) and sugar pine (*Pinus lambertiana*); other less common associates include incense cedar (*Calocedrus decurrens*) and lodgepole pine (*Pinus contorta*) (Minnich 2000). Jeffrey pine is closely related to ponderosa pine, and replaces it in drier, colder, and/or pedologically challenging situations (Safford and Stevens, in press). Soils are predominantly granitic, and climate is Mediterranean with summer monsoonal influences; ecologically significant climate trends (e.g. mean minimum temperature in January, mean maximum temperature in July, average total precipitation) in the SSPM have historically fallen within the range of variation observed in the eastern Sierra Nevada (Dunbar-Irwin and Safford 2016). The reference fire regime in the SSPM is also very similar to that described for the yellow pine and mixed conifer forests in California, with a median fire return interval of about 15 years (Stephens et al. 2003), compared to 7-12 years in California (van de Water and Safford 2011); in both regions, intact fire regimes typically exert low and moderate severity fire effects are usually observed when f (Rivera et al. 2016).

Objective 1 – Determining a Recommended Minimum Tree-height Cutoff

Identifying Tree Locations

Field Data: Tree diameter, height, and location (UTM coordinates) data were measured in the field by Fry and others (2014) using state-of-the art stem mapping techniques on two 4-ha plots located within the SSPM LiDAR acquisition (Fig. 1). These precise, high-resolution datasets capture actual conditions and were used as the standard for accuracy assessments of LiDAR-based structural analyses.

LiDAR Data: E W Wells Group, LLC collected discrete point-return LiDAR data over 6,440 hectares in the SSPM on November 28th, 2015 (acquisition boundary shown in Figure 1), using a Leica ALS80 system mounted on a Cessna 208B Caravan flying at 1800m altitude. The Leica ALS80 system emitted 8 pulses/m^2, with an ability to receive unlimited return pulses; the acquisition achieved an average of 14.82 first returns and 3.34 ground returns per m^2.

To determine individual tree locations, a tree segmentation process was run on a canopy height model (continuous raster of the top layer of vegetation derived from the SSPM LiDAR point cloud) using FUSION'S TreeSeg tool (data processing performed by Dr. Van Kane). TreeSeg delineates distinct vegetation features from the canopy height model and applies a watershed segmentation algorithm to identify the highest point of each vegetation feature; high points are then interpreted as individual trees (McGaughey 2016). TreeSeg is a free, widely-available tool in FUSION's software package and the watershed segmentation process is commonly used in ITD studies (Jeronimo 2015). For all trees detected by TreeSeg, I used location and height data to predict individual tree diameters. Predictions were based on a randomForest model (pseudo-R^2 = 83.7%) built with diameter, height, and location data from more than 3,000 field-measured trees located across the study area (Liaw and Weiner 2002).

Comparing Number of Remaining Trees, Spatial Maps, and Estimates of Structure and Spatial Pattern

After extracting LiDAR-detected trees from within the Fry (field-measured) plots, I removed trees less than 6 m, 9 m, 12 m, 15 m, and 18 m tall (i.e. increased minimum height cutoff of trees used in analyses) from both field and LiDAR datasets. I compared the number of trees remaining, spatial tree density maps, and structural estimates between these five pairs of datasets, with the expectation that agreement between field and LiDAR data would improve as minimum height cutoff increased. There were only two field sites; the ridge plot, on metamorphic soils, supported nearly twice as many trees as the shallow southerly (SHS) plot. This extreme difference in stand density precluded a meaningful statistical comparison of the two and as a result, I analyzed the Fry plots separately.

Number of Remaining Trees: Because most understory trees will not be identified by TreeSeg or other ITDs, we expect there to be fewer LiDAR-detected than field-measured trees within a given area (in this case, the 4-ha Fry plots). Although increasing the minimum height cutoff will reduce the number of trees remaining in both datasets, the extent of this reduction is probably different for LiDAR and field tree lists, and for low- and high-density stands. I tallied the number of field-measured and LiDAR-detected trees remaining in datasets and the differences between them as trees in lower height classes were removed.

Spatial Tree Density Maps: I converted point pattern maps made using field and LiDAR tree location data into pairs of point density rasters such that the value of each pixel corresponded to the number of trees located within. I used the vegan package in R to apply partial Mantel tests to dissimilarity matrices quantifying (Euclidean) pairwise distances between all pixel pairs in each raster. Partial Mantel tests employ a third dissimilarity matrix of Euclidean pairwise distances between pixel coordinates; this matrix controls for potential effects of spatial autocorrelation, an important consideration when comparing two maps of the same geographical area. For the tests, field- and LiDAR-based matrices were separately regressed against the Euclidean distance matrix and the Mantel test score was calculated as the correlation between residuals of the two regressions. Partial Mantel tests were repeated for all five field and LiDAR pairs of 6 m, 9 m, 12 m, 15 m, and 18 m tree datasets.

In addition to assessing the relationship between height and spatial correlation, I investigated the effect of scale on agreement in the location and number of trees between the two data sources by comparing partial Mantel scores at different levels of pixel aggregation (i.e. area on the ground). Very fine spatial scales were not assessed because a lack of vertical alignment between tree bases (coordinates measured at ground-level in the field) and crowns (coordinates measured by LiDAR from above) and spatial measurement error of each leads us to expect that LiDAR-detected and field measured trees will often be located 2m or more apart (Vauhkonen et al. 2012). Although increasing the spatial grain should improve partial Mantel correlations, areas larger than the average size of tree clumps in Fry plots (48.6 to 316.2 m^2; Fry et al. 2014) lack management relevance and were excluded from this analysis.

Estimates of Forest Structure and Spatial Pattern: For all field-and LiDAR minimum height datasets, I generated estimates of five stand-level structure variables and 23 spatial pattern variables. By graphing the difference in estimates, I was able to visually assess the effect of minimum tree height on the accuracy of LiDAR-based forest structure estimates.

Stand-level structure variables were calculated using all trees in each minimum height dataset and included basal area (BA; summed area of all tree cross-sections) per hectare, number of trees per hectare (TPH), average tree diameter, average tree height, and mean clump size (MCS) (average number of trees per clump). To assess spatial pattern, I identified tree clumps using Plotkin's (2002) algorithm, which assigns trees within a defined distance of each other (i.e. inter-tree distance) to the same clump. Clump size classes (CSC's) were defined as individual trees (trees lacking neighbors within the inter-tree distance), small clumps (2-4 trees), medium clumps (5-9 trees), and large clumps (10 or more trees). The average crown radius of mature ponderosa pine in western North America is 3 m; given the similarities among SSPM forests and those of western North America, I selected 6 m as the constant inter-tree distance (Lydersen et al. 2013; Churchill et al. 2015; Clyatt et al. 2015). Clumping analyses were carried out in R, using spatstat (Baddeley et al. 2015) and sp (Pebesma and Bivand 2005) packages. The variables analyzed for each CSC were basal area (BA) per hectare, BA per clump, tree density (number of trees per hectare), number of clumps per hectare (except for individual trees); average diameter; and average height.

Objective 2 – Testing the Ability of LiDAR-Detected Trees Above a Minimum Height to Capture Structural Variation

Landform Characterization

Using the Land Management Unit tool (North et al. 2012), I divided the study area into six landforms: canyons, ridges, northerly and southerly slopes >30% steepness, and northerly and southerly slopes <30% steepness (Table 1; Figure 1). The 30% criterion was used because slopes steeper than this are often subject to higher severity fires than shallow slopes and are liable to be structurally distinct; in addition, thinning and other management activities are limited on steep slopes (North et al. 2012).

For four of the six landforms (ridges, canyons, and shallow northerly and southerly slopes), I extracted contiguous areas greater than 10 ha in size. To accommodate processing limitations, I manually converted these areas into polygons with smooth boundaries up to 90 ha in size (Table 1; Figure 1). The other two landforms (steep northerly and southerly slopes) each comprise less than 5% of the study landscape; due to limited representation, the minimum size for polygons of these landforms was reduced to 4ha.

Within each polygon, I used LiDAR-detected trees above the recommended height cutoff to calculate 5 stand-level average and 23 spatial pattern variables (methods described above). In addition to multi- and uni-variate statistical tests of differences among landforms, I constructed side-by-side boxplots depicting variation in the distributions of variable estimates according to landform and produced tables reporting the interquartile range and means of all variables for each landform.

Multivariate Analyses

I assessed structural differences among landforms using non-metric multidimensional scaling (NMDS) (McCune and Grace 2002). For this study, landforms were analogous to community types, sample areas were analogous to sites, and the 28 structure variables were analogous to species in community ecology studies, where NMDS is most commonly employed. I used the metaMDS function in the vegan package (Oksanen et al. 2016) in R to carry out the ordination with jaccard as the distance measure, 500 random starts, and a maximum of 200 iterations, then calculated and plotted the mean and the standard error of the axis scores for each landform. In ordination plots, structurally similar landforms are clustered while dissimilar landforms are separated (McCune and Grace 2002).

To test for significant differences among landforms based on all variables, I used the vegan package in R to conduct a multi-response permutation procedure (MRPP) to compare variation within and among groups (groups = landforms, weighted by sample size), using a city-block distance matrix to calculate the weighted-mean within-group distance (δ). The test randomly assigned observations to groups over 999 Monte Carlo permutations, calculating a new δ and comparing it to the observed δ for each permutation. Among-group differences are statistically significant if the observed δ is lower than δs of randomly permuted groups. The MRPP test statistic A describes within-group homogeneity; a score of 1 indicates all observations in groups are the same, while a score of 0 indicates perfect heterogeneity within groups (McCune and Grace, 2002).

Univariate Comparisons

Data were unbalanced, contained a mix of normal and non-normal distributions, and variances among variables and groups of variables were unequal. I performed Dunnett's modified Tukey-Kramer multiple pairwise comparisons (DTK package in R ((Lau 2013)) on all variables. These pairwise comparisons calculate confidence intervals for the difference between ranked means of all 15 landform pairs; if confidence intervals did not contain 0, landform pairs were considered to be significantly different.

Results

Objective 1 – Determining a Recommended Minimum Tree Height Cutoff

Number of Remaining Trees: When no tree-height cutoff was applied, TreeSeg detected only 36% of the trees on the ridge plot. In contrast, TreeSeg detected 72% of field-measured trees on the shallow southerly (SHS) plot where tree density was much lower (757 vs. 1486 trees, respectively) (Table 2, Fig. 2).

In the denser ridge plot, increasing the minimum height cutoff by 3 m increments up to 15 m strongly reduced the difference in number of field-measured and LiDAR-detected trees (963 vs. 29, Table 2); at this height cutoff, the number of LiDAR-detected trees was 91% of the number of field-measured trees

(Fig. 2). On the SHS plot, there was a similar trend through the 12 m height cut off, where the difference in tree numbers was reduced from 211 to 14 and the number of LiDAR-detected trees was 97% of the number of field-measured trees (Table 2, Figure 2).

Spatial Tree Density Maps: Regardless of minimum tree-height cutoff, there was low agreement between field and LiDAR density maps at the smallest spatial scale considered (9.77 m^2; 3.125 x 3.125 m); correlations coefficients were lower on the SHS than the ridge plot (< 0.06 and 0.23, respectively) (Supplementary Appendix Fig. 1; p-value for all correlations = 0.001). Aggregating pixels into larger areas increased correlation scores on both plots (Supplementary Appendix Fig. 1). In 6.25 by 6.25 m areas (39.0625 m^2), correlation of local tree density estimates increased to almost 0.3 (for trees > 15 m tall) on the SHS plot and to just over 0.45 (for trees > 11 m) on the ridge plot; in 12.5 by 12.5 m areas (156.25 m^2), correlations reached 0.57 (trees > 15 m) on the SHS plot and 0.62 (trees > 14 m) on the ridge plot. Correlation coefficients did not increase when the height cutoff increased from 15 to 18 m on either plot.

Estimates of Forest Structure and Spatial Pattern: Increasing the minimum height cutoff reduced differences between LiDAR-and field-based estimates of spatial pattern (Fig. 3) and of stand-level forest structure in particular (Fig. 4). Estimate discrepancies remained large for the 6 and 9 m height cutoffs and were generally much smaller for the low-density (SHS) than the high-density (ridge) plot (Fig.'s 3 and 4).

The 18 m height cutoff minimized the differences between LiDAR-and field-based estimates of tree density, mean clump size, and BA per hectare estimates on both plots (Fig. 4). However, no large clumps were identified using LiDAR or field data on either plot at the 18 m cutoff; large clumps were also absent from LiDAR datasets at the 15 m cutoff, which negatively affected the accuracy of large clump metrics (Fig. 3).

For some metrics, the 12 m height cutoff was most accurate, while for others, the 15 m cutoff was superior. In addition, the direction and magnitude of estimate differences at 12 and 15 m height cutoffs varied between plots (Fig. 3). For example, on the ridge plot, small clump density was slightly overestimated at the 12 m cutoff but was underestimated to a larger degree at 15 m (0.6 and -2.6 clumps/ha, respectively) (Fig. 3a). In contrast, increasing the cutoff from 12 to 15 m on the SHS plot changed the estimate difference from 2 to -0.6 small clumps/ha (Fig. 3a). Similar trends are evident for estimates of the number of trees per hectare in each CSC; however, the density of individual trees was overestimated and the average diameter and height of individuals was underestimated on both plots at both height cutoffs (Fig. 3b, Supplementary Appendix Fig. 2a, 2b). Although the difference in estimates of BA/ha of each CSC were slightly lower at the 15 than the 12 m cutoff, BA per large clump (Fig. 3d) and average diameter and height of trees in large clumps (Supplementary Appendix Fig. 2) for the 15 m cutoff were strongly underestimated relative to the 12 m datasets.

Estimate differences for nearly all structure and spatial variables on the SHS plot were minimally affected by increasing the height cutoff from 12 to 15 m, and at the 15 m cutoff, plot-level tree density on the SHS plot was overestimated. Multiple lines of evidence suggest that a 12 m height cutoff is appropriate for using LiDAR and ITD to characterize forest structure and spatial pattern in low-density, open-canopy forest types such as those of the Fry SHS plots. For these reasons, I selected 12 m height cutoff in the characterization of structural conditions across the reference landscape.

Objective 2 – Testing the Ability of LiDAR-Detected Trees Above a Minimum Height to Capture Structural Variation

Multivariate Analyses

Considering all variables simultaneously for trees > 12 m tall, there was significant variation among landforms (A = 0.15; observed δ = 76.07, less than the expected δ of 89.04; p-value = 0.001). Canyons, shallow northerly slopes, and shallow southerly slopes clustered together. While not nearly as close together, steep southerly slopes and ridges were separated along Axis 1 from the other landforms, while Steep northerly slopes were in between clusters of the other landforms (Fig. 5).

Univariate Analyses

Variables describing large clumps were not significantly different between any landform pairs (data not shown). The number of medium clumps and number of trees in medium clumps was slightly but significantly lower on steep and shallow southerly slopes than on steep northerly slopes, however, these and other medium clump variables were generally not statistically different between landforms. Mean clump size was only significantly different between steep northerly and steep southerly slopes (~ 0.42 more trees per clump on steep northerly than southerly slopes) (Table 3).

In contrast, the remaining structure and spatial pattern variables were usually significantly different between at least four (out of 15 total) landform pairs (Table 3). There were fewer trees and clumps, and the trees were smaller on steep southerly slopes and ridges than on the other four landforms (Fig.'s 6 and 7). Structure and spatial pattern variables were generally not different among canyons, shallow northerly slopes, and shallow southerly slopes, or between ridges and steep southerly slopes. For example, BA/ha of all trees pooled was 8.7 m^2 higher on canyons and shallow northerly slopes, 6 m^2 higher on steep northerly slopes, and 7 m^2 higher on shallow southerly slopes than on steep southerly slopes. However, BA/ha of all trees pooled was not statistically different between steep southerly slopes and ridges, or among shallow slopes, canyons, and steep northerly slopes (Table 3).

Structure on steep northerly slopes did not follow a regular pattern: in some cases, variable estimates were statistically different from ridges and steep southerly slopes and not different from canyons and shallow slopes, and in other cases the opposite was true. For example, the average height of individual trees on steep northerly slopes was significantly lower than on canyons and shallow northerly slopes (by 2.4 and 2 m, respectively), was not different from shallow or steep southerly slopes, and was significantly greater than on ridges (by 2.3 m) (Table 3).

Discussion

My study is one of the first to quantify variation in forest structure across a modern reference landscape at multiple spatial scales using widely-available methods. Despite LiDAR's obvious benefits, including high resolution at multiple spatial scales, extensive spatial coverage, robust replication potential, and cost-efficiency, managers and researchers have been reluctant to use it for structural characterizations of complex, heterogeneous forests, because sub-dominant trees are rarely detected and there is low confidence in ITD's ability to approximate actual tree distributions (Kaartinen et al. 2012, Falkowski et al. 2008). However, my results bolster a growing body of literature supporting the reliability of ITD-based stand-level structure and spatial pattern estimates when minimum height cutoffs are applied (Jeronimo

2015, Richardson and Moslak 2012). By applying minimum height cutoffs to LiDAR-detected trees, I captured fine-scale heterogeneity and accurately identified tree clumps of different sizes, structures that can be linked to forest resiliency and the integrity of ecological processes (Larson and Churchill 2012, Lydersen et al. 2013, Fry et al. 2014). In contrast to other LiDAR-based analyses, my approach provides explicit descriptions of overstory tree arrangements and directly applies to the development of management prescriptions (Kaartinen et al. 2012, Li et al. 2012). In addition, this method avoided biases (e.g. limited spatial extent, lack of representation, low replication) of the field-based historic stand reconstructions that are increasingly used for reference model construction (Stephens et al. 2015, Kane et al. 2014). Finally, my results indicate that considering landscape context is essential in the development of reference models for forest management and restoration, and that LiDAR can meet these needs if inherent weaknesses are addressed.

ITD inaccuracies are well-documented and can be split into omission (failure to detect trees that are actually present) and commission (detecting trees that are not actually present) errors (Breidenbach 2010). Omission rates increase significantly with relative tree height, canopy cover, stand density, and tree clustering, and are often greater than commission error rates; in contrast, false tree detections usually occur in low-density, open-canopy stands where older trees develop complex crown shapes with several high points (Jeronimo 2015, Falkowski et al. 2008, Vauhkonen et al. 2012). For example, Falskowski et al. (2008) reported very low omission rates (4 – 8%) but increased commission rates (12 – 17%) in forests with low canopy cover (0 – 25%) relative to those with closed canopies. The same authors also found that excluding sub-dominant trees from assessments of ITD accuracy reduces omission but increases commission errors.

In this study, omission rates declined as the minimum height cutoff increased, and the effect was stronger on the ridge than on the SHS plot. Commission error was evident on the SHS plot once the height cutoff exceeded 12 m; there were more LiDAR-detected than field-measured trees for 15 and 18 m cutoffs. For this low-density SHS plot, a 12 m height cutoff reduced omission errors while capturing more medium and large clumps than the 15 m dataset; in addition, estimate differences were not strongly affected by increasing minimum tree height from 12 to 15 m. The ridge and SHS plots varied starkly in terms of stand density but canopy cover was not significantly different (Fry et al. 2014) and a large body of research indicates that ITD will always perform poorly in closed-canopy stands (Falkowski et al. 2008, Vauhkonen et al. 2012). The 15 m cutoff may be more appropriate in higher density stands, however, it should be applied cautiously with the understanding that medium and large clump frequencies may be significantly underestimated and that success is unlikely in forests with high canopy cover.

Along with density effects, the accuracy of stand-level versus spatial pattern and spatial tree density estimates varied with minimum height cutoff. Stand-level estimates of tree density, size, and basal area were most accurate for trees greater than 18 m tall. Richardson and Moskal (2011) also produced reliable density estimates for trees greater than 20 m tall using LiDAR and ITD. Increasing the height cutoff improved agreement between field and LiDAR tree density spatial maps up to a point; however, the effects of spatial scale were considerably stronger than those of minimum tree height, and the correlations did not improve when the height cutoff exceeded 15 m. It was surprising to find higher partial Mantel correlations on the high-density ridge than the SHS plot. One possible explanation is that differences in tree density were large but concentrated within few, relatively small areas on the ridge plot, but were widespread and frequent on the low-density SHS plot, leading to common and consistent disagreements in local tree density.

The 18 m height cutoff was better for stand-level characterizations, however, it was unable to accurately describe spatial pattern, because it eliminated large clumps from field and LiDAR datasets; spatial pattern estimates for the 12 and 15 m cutoffs were clearly more accurate. However, omission errors limited LiDAR's ability to produce reliable estimates of small, medium, and large clumps at all height cutoffs on both plots. Even when datasets were trimmed and smaller tree size classes were removed, tall trees growing underneath the dominant canopy were captured in field stem maps but not by the TreeSeg algorithm. On the ridge plot, trees in small and medium clumps were misclassified as individuals, inflating LiDAR-derived estimates of individual tree BA/ha, as well as the number of individual trees. Similarly, LiDAR overestimated the frequency (and consequently, BA/ha) of small clumps on the SHS plot because understory trees of medium and large clumps measured in the field were not detected. Since the size of many trees misclassified as individuals was actually constrained by close neighbors and clump membership, the average diameter and height of individual trees was underestimated on both plots.

Despite these shortcomings, I found strong evidence that LIDAR, with an appropriate tree-height cut off (in this case 12 m), can be used to accurately assess structural variation across the SSPM, a reference landscape dominated by open-canopy forest types. Average canopy cover in my reference landscape was 25.3%, on the threshold for minimum omission rates observed by Falkowski et al. (2008). Canyons, shallow northerly slopes, and shallow southerly slopes appeared structurally similar to one another, as did steep southerly slopes and ridges; in contrast, steep northerly slopes exhibit structural distinctions. These findings were corroborated by the univariate analyses, which detected significantly fewer, smaller trees and clumps on steep southerly slopes and ridges than on the other four landforms. Previous studies in the Sierra Nevada and Klamath Mountains of the western US also have found that stand density, canopy cover, and basal area tends to be greatest in canyons and lowest on ridges (Taylor and Skinner 2003; Lydersen and North 2012; Underwood et al. 2010).

Variation among landforms can be attributed to topographical control over forest structure (and fire regimes) in mountainous regions. Slope position, aspect, and steepness interact with climate to create moisture and temperature gradients that significantly affect vegetation and fire behavior (Perry et al. 2011, Dillon et al. 2011). In mountainous landscapes, topography also controls the fine-scale distribution and combustibility of fuels; for example, ridges and steep slopes tend to have higher fire intensities, lower moisture availability, and shallower soils than other landforms (Beaty and Taylor 2001, Urban et al. 2000). Northerly aspects are more prone to high-severity fires because they support large fuel loadings, while southerly aspects are more exposed to radiation and heat, which are associated with high fuel drying rates, longer fire seasons, and increased fire likelihoods (Holden et al. 2009, Dillon et al. 2011, Miller and Urban 2000).

In the SSPM, structure and spatial pattern on shallow northerly and southerly slopes was not significantly different. This region is drier than the western Sierra Nevada and the Klamath mountains, which may dampen the usual effect of slope aspect such that water balance, vegetation, and disturbance history is similar on shallow slopes of all aspects. However, on steep slopes, aspect does appear to be a significant driver of structural variation. For example, median BA/ha and TPH on steep northerly slopes was 13.7 m^2 and 56.3, compared to 7.9 m^2 and 36.6 on steep southerly slopes, respectively (Supplementary Appendix).

In addition to conforming to previous assessments of structural variation by landform, my findings are also consistent with those from other characterizations of reference conditions in yellow pine and mixed-conifer forests of western North America. In my LiDAR estimates, average TPH and BA/ha across all

landforms was 48 and 13.2 m^2, respectively (Supplementary Appendix). Also in SSPM, Stephens and Gill (2005) measured 145 TPH and 20 m^2/ha BA in a locally intensive field-sampled dataset (all trees >2.5 cm dbh), and Dunbar-Irwin and Safford (2016) measured 187 TPH and 22.5 m^2/ha in a spatially extensive field-sampled dataset (all trees >7.5 cm dbh). In a review of the natural range of variation (NRV) in yellow pine and mixed conifer forests in the mountains of eastern California (southern Cascades, Modoc Plateau, Sierra Nevada, White and Inyo Mountains), Safford and Stevens (in press) report an overall reference average of 159 TPH (range of means from many studies for trees >10 cm dbh = 60-328), and an overall reference average BA/ha of 35 m^2 (range 20-54); reference data were from early settlement estimates, reference landscapes with intact fire regimes, and stand reconstructions. From the southwestern US, Stoddard (2011) reports a reference average BA/ha of 16 m^2, and Reynolds and others (2013) write that historic TPH was 30-315 and 53-251 in ponderosa pine and mixed-conifer forests, respectively. Overall, my SSPM estimates fall below the lower range of estimates from both SSPM itself and the larger region. This is due to the exclusion of trees below 12 m height and underlines the challenges of using LiDAR to estimate standard forest structural conditions like TPH and BA, even in relatively sparse canopy stands.

Management Implications

Characterizing forest structure and spatial pattern in reference ecosystems for distinct landforms allows managers to tailor their restoration prescriptions according to the physical location of project areas. Restoring site-specific structure and spatial heterogeneity may increase landscape resiliency by re-establishing feedbacks between disturbance and vegetation dynamics and other self-regulating processes that may have been broken down by long histories of logging and fire-suppression (Larson and Churchill 2012; Parks et al. 2015). Landform classes used in this study successfully divided the SSPM into like units that were structurally distinct, indicating that this strategy is a viable framework for management. A digital elevation model is the only requirement for using the Landscape Management Tool to separate landscapes into landform classes; in addition, FUSION's TreeSeg tool is widely available and this strategy can be adopted by managers everywhere.

If managers are interested in using LiDAR and TreeSeg to describe current or reference structural conditions, increasing the minimum height cutoff of LiDAR tree datasets can generate reasonable estimates of overstory spatial pattern and forest structure. Most above-ground biomass in forests is generally contained in dominant, overstory trees; large trees are also significant forest carbon sinks and are crucial habitat components for a range of wildlife species (Jeronimo 2015). The arrangement of overstory trees may be a significant component of spatial heterogeneity in forested landscapes, and using trees > 12 m tall, I was able to accurately describe that arrangement and how it varies across landforms. However, LiDAR-detected trees will always underestimate the frequency of small, medium, and large tree clumps. This limitation will be more pronounced in high-density stands and, therefore, my approach is most suitable for use in open-canopy, low-density forest types.

This research emphasizes the need for understanding structural variation at multiple spatial scales. Landforms are structurally distinct and applying reference information from forests of one landform to forests of another is unlikely to achieve management goals. In addition, stand-level averages are incapable of describing structural heterogeneity and their use in reference models should be avoided. The approach developed here overcomes many important limitations of forest reference models and the results may be used to inform restoration in dry fire-dependent forests of western North America and similar forest types across the globe.

References

Abella, Scott R., and Charles W. Denton. "Spatial variation in reference conditions: historical tree density and pattern on a *Pinus ponderosa* landscape." *Canadian Journal of Forest Research* 39.12 (2009): 2391-2403.

Baddeley, Adrian, Ege Rubak, and Rolf Turner (2015). Spatial Point Patterns: Methodology and Applications with R. London: Chapman and Hall/CRC Press, 2015. http://www.crcpress.com/Spatial-Point-Patterns-Methodology-and-Applications-with-R/Baddeley-Rubak-Turner/9781482210200/

Beaty, R. Matthew, and Alan H. Taylor. "Spatial and temporal variation of fire regimes in a mixed conifer forest landscape, Southern Cascades, California, USA." *Journal of Biogeography* 28.8 (2001): 955-966.

Bivand, Roger and Colin Rundel (2016). rgeos: Interface to Geometry Engine - Open Source (GEOS). R package version 0.3-20. https://CRAN.R-project.org/package=rgeos

Bivand, Roger, Tim Keitt and Barry Rowlingson (2016). rgdal: Bindings for the Geospatial Data Abstraction Library. R package version 1.1-10. https://CRAN.R-project.org/package=rgdal

Breidenbach, Johannes, et al. "Prediction of species specific forest inventory attributes using a nonparametric semi-individual tree crown approach based on fused airborne laser scanning and multispectral data." *Remote Sensing of Environment* 114.4 (2010): 911-924.

Churchill, Derek J. et al. Historical forest structure, composition, and spatial pattern in dry conifer forests of the western Blue Mountains, Oregon. USDA Forest Service PNW Research Station General Technical Report PNW-GTR-XXXX. (2015) In press.

Churchill, Derek J., et al. "Restoring forest resilience: from reference spatial patterns to silvicultural prescriptions and monitoring." *Forest Ecology and Management* 291 (2013): 442-457.

Dillon, Gregory K., et al. "Both topography and climate affected forest and woodland burn severity in two regions of the western US, 1984 to 2006." *Ecosphere* 2.12 (2011): 1-33.

Dobrowski, Solomon Z. "A climatic basis for microrefugia: the influence of terrain on climate." *Global change biology* 17.2 (2011): 1022-1035.

Dunbar-Irwin, Mila, and Hugh Safford. "Climatic and structural comparison of yellow pine and mixed-conifer forests in northern Baja California (México) and the eastern Sierra Nevada (California, USA)." *Forest Ecology and Management* 363 (2016): 252-266.

Falkowski, Michael J., et al. "The influence of conifer forest canopy cover on the accuracy of two individual tree measurement algorithms using lidar data." *Canadian Journal of Remote Sensing* 34.S2 (2008): S338-S350.

Franklin, Jerry F., and K. Norman Johnson. "A restoration framework for federal forests in the Pacific Northwest." *Journal of Forestry* 110.8 (2012): 429-439.

Fry, Danny L., et al. "Contrasting spatial patterns in active-fire and fire-suppressed Mediterranean climate old-growth mixed conifer forests." *PloS one* 9.2 (2014): e88985.

Harrell, Frank E Jr, with contributions from Charles Dupont and many others. (2016). Hmisc: Harrell Miscellaneous. R package version 3.17-4. https://CRAN.R-project.org/package=Hmisc

Hessburg, Paul F., et al. "Restoring fire-prone Inland Pacific landscapes: seven core principles." *Landscape Ecology* 30.10 (2015): 1805-1835.

Hessburg, Paul F., R. Brion Salter, and Kevin M. James. "Re-examining fire severity relations in pre-management era mixed conifer forests: inferences from landscape patterns of forest structure." *Landscape Ecology* 22.1 (2007): 5-24.

Hijmans, Robert J. (2016). raster: Geographic Data Analysis and Modeling. R package version 2.5-8. https://CRAN.R-project.org/package=raster

Holden, Zachary A., Penelope Morgan, and Jeffrey S. Evans. "A predictive model of burn severity based on 20-year satellite-inferred burn severity data in a large southwestern US wilderness area." *Forest Ecology and Management* 258.11 (2009): 2399-2406.

Kaartinen, Harri, et al. "An international comparison of individual tree detection and extraction using airborne laser scanning." *Remote Sensing* 4.4 (2012): 950-974.

Kane, Van R., et al. "Landscape-scale effects of fire severity on mixed-conifer and red fir forest structure in Yosemite National Park." *Forest Ecology and Management* 287 (2013): 17-31.

Kane, Van R., et al. "Patch dynamics and the development of structural and spatial heterogeneity in Pacific Northwest forests." *Canadian Journal of Forest Research* 41.12 (2011): 2276-2291.

Kane, Van R., et al. "Water balance and topography predict fire and forest structure patterns." *Forest Ecology and Management* 338 (2015): 1-13.

Larson, Andrew J., and Derek Churchill. "Tree spatial patterns in fire-frequent forests of western North America, including mechanisms of pattern formation and implications for designing fuel reduction and restoration treatments." *Forest Ecology and Management* 267 (2012): 74-92.

Lau, Matthew K. (2013). DTK: Dunnett-Tukey-Kramer Pairwise Multiple Comparison Test Adjusted for Unequal Variances and Unequal Sample Sizes. R package version 3.5. https://CRAN.RProject.org/package=DTK

Li, Wenkai, et al. "A new method for segmenting individual trees from the lidar point cloud. "*Photogrammetric Engineering & Remote Sensing* 78.1 (2012): 75-84.

Liaw, A. and M. Wiener (2002). Classification and Regression by randomForest. R News 2(3), 18--22.

Lydersen, Jamie M., et al. "Quantifying spatial patterns of tree groups and gaps in mixed-conifer forests: reference conditions and long-term changes following fire suppression and logging." *Forest Ecology and Management* 304 (2013): 370-382.

Lydersen, Jamie, and Malcolm North. "Topographic variation in structure of mixed-conifer forests under an active-fire regime." *Ecosystems* 15.7 (2012): 1134-1146.

Mcdonald, Tein et al. (2016). International standards for the practice of ecological restoration–including principles and key concepts. Society for Ecological Restoration

Meyer, Marc D., et al. "Influence of soil thickness on stand characteristics in a Sierra Nevada mixed-conifer forest." *Plant and Soil* 294.1-2 (2007): 113-123.

Miller, Carol, and Dean L. Urban. "Modeling the effects of fire management alternatives on Sierra Nevada mixed-conifer forests." *Ecological Applications* 10.1 (2000): 85-94.

Milodowski, David T., Simon M. Mudd, and Edward TA Mitchard. "Erosion rates as a potential bottom-up control of forest structural characteristics in the Sierra Nevada Mountains." *Ecology* 96.1 (2015): 31-38.

Minnich, Richard A., et al. "Californian mixed-conifer forests under unmanaged fire regimes in the Sierra San Pedro Mártir, Baja California, Mexico." *Journal of Biogeography* 27.1 (2000): 105-129.

North, Malcolm, et al. "An ecosystem management strategy for Sierran mixed-conifer forests." (2009).

North, Malcolm. "Managing Sierra Nevada forests." (2012).

Oksanen, Jari, F. Guillaume Blanchet, Michael Friendly, Roeland Kindt, Pierre Legendre, Dan McGlinn, Peter R. Minchin, R. B. O'Hara, Gavin L. Simpson, Peter Solymos, M. Henry H. Stevens, Eduard Szoecs and Helene Wagner (2016). vegan: Community Ecology Package. R package version 2.4-1. https://CRAN.R-project.org/package=vegan

Parks, S.A., L. M. Holsinger, C. Miller, and C.R. Nelson. 2015. Wildfire as a self-regulating mechanism: the role of previous burns and weather in limiting fire progression. *Ecological Applications* 25:1478–1492.

Pebesma, E.J., R.S. Bivand, 2005. Classes and methods for spatial data in R. R News 5 (2), http://cran.r-project.org/doc/Rnews/.

Perry, David A., et al. "The ecology of mixed severity fire regimes in Washington, Oregon, and Northern California." *Forest Ecology and Management* 262.5 (2011): 703-717.

Plotkin, Joshua B., Jérôme Chave, and Peter S. Ashton. "Cluster analysis of spatial patterns in Malaysian tree species." *The American Naturalist* 160.5 (2002): 629-644.

Richardson, Jeffrey J., and L. Monika Moskal. "Strengths and limitations of assessing forest density and spatial configuration with aerial LiDAR." *Remote Sensing of Environment* 115.10 (2011): 2640-2651.

Richardson, Jeffrey J., and L. Monika Moskal. "Strengths and limitations of assessing forest density and spatial configuration with aerial LiDAR." *Remote Sensing of Environment* 115.10 (2011): 2640-2651.

Rivera-Huerta, Hiram, Hugh D. Safford, and Jay D. Miller. “Patterns and trends in burned area and fire severity 1984-2010 in the Sierra de San Pedro Mártir, Baja California, México.” *Fire Ecology* 12 (2016): 52-72.

Safford, Hugh D., and Jens T. Stevens. “Natural Range of Variation (NRV) for yellow pine and mixed conifer forests in the Sierra Nevada, southern Cascades, and Modoc and Inyo National Forests, California, USA.” General Technical Report PSW-GTR-256, USDA Forest Service, Pacific Southwest Research Station, Albany, CA. In press.

Sánchez Meador, Andrew J., Pablo F. Parysow, and Margaret M. Moore. "A new method for delineating tree patches and assessing spatial reference conditions of ponderosa pine forests in northern Arizona." *Restoration Ecology* 19.4 (2011): 490-499.

Schoennagel, Tania, and Cara R. Nelson. "Restoration relevance of recent National Fire Plan treatments in forests of the western United States." *Frontiers in Ecology and the Environment* 9.5 (2011): 271-277.

Society for Ecological Restoration International Science & Policy Working Group, 2004. *The SER International Primer on Ecological Restoration*. www.ser.org & Tucson: Society for Ecological Restoration International.

Stephens, Scott L., and Peter Z. Fulé. "Western pine forests with continuing frequent fire regimes: possible reference sites for management." *Journal of Forestry* 103.7 (2005): 357-362.

Stephens, Scott L., and Samantha J. Gill. "Forest structure and mortality in an old-growth Jeffrey pine-mixed conifer forest in north-western Mexico." *Forest Ecology and Management* 205.1 (2005): 15-28.

Stephens, Scott L., et al. "Historical and current landscape-scale ponderosa pine and mixed conifer forest structure in the Southern Sierra Nevada." *Ecosphere* 6.5 (2015): 1-63.

Swetnam, Thomas W., Craig D. Allen, and Julio L. Betancourt. "Applied historical ecology: using the past to manage for the future." *Ecological applications* 9.4 (1999): 1189-1206.

Taylor, Alan H., and Carl N. Skinner. "Spatial patterns and controls on historical fire regimes and forest structure in the Klamath Mountains."*Ecological Applications* 13.3 (2003): 704-719.

Underwood, Emma C., et al. "Using topography to meet wildlife and fuels treatment objectives in fire-suppressed landscapes." *Environmental management* 46.5 (2010): 809-819.

Urban, Dean L., et al. "Forest gradient response in Sierran landscapes: the physical template." *Landscape Ecology* 15.7 (2000): 603-620.

Van de Water, Kip M., and Hugh D. Safford. "A summary of fire frequency estimates for California vegetation before Euroamerican settlement." *Fire Ecology* 7.3 (2011): 26-58.

Vauhkonen, Jari, et al. "Comparative testing of single-tree detection algorithms under different types of forest." *Forestry* 85.1 (2012): 27-40.

Tables

	Canyon	Shallow N	Steep N	Ridge	Shallow S	Steep S
n	18	28	21	26	36	20
Mean Area (ha)	39	43	11	20	38	13
Total Area (ha)	709	1196	226	508	1352	255

Table 1. Number of sample areas (polygons), average size of sample areas, and the total area sampled in each landform. N stands for northerly, and S stands for southerly; shallow refers to slopes less than or equal to 30%, and steep refers to slopes greater than 30%.

Dataset	Number of Field Trees (Percent of Total)	Number of LiDAR Trees (Percent of Total)	Difference in Number of Field and LiDAR Trees
Ridge			
All Trees	1486 (100%)	523 (100%)	963
Trees > 6m	931 (63%)	476 (91%)	455
Trees > 9m	680 (46%)	436 (83%)	244
Trees > 12m	481 (32%)	384 (73%)	97
Trees > 15m	318 (21%)	289 (55%)	29
Trees > 18m	213 (14%)	190 (36%)	23
Shallow Southerly			
All Trees	757 (100%)	546 (100%)	211
Trees > 6m	574 (76%)	470 (86%)	104
Trees > 9m	493 (65%)	431 (79%)	62
Trees > 12m	407 (54%)	393 (72%)	14
Trees > 15m	345 (46%)	360 (66%)	-15
Trees > 18m	268 (35%)	302 (55%)	-34

Table 2. Change in number (and percent) of trees in field and LiDAR datasets, and the difference in number of trees between field and LiDAR datasets, as trees below specific height cutoffs are removed. For example, refer to the bottom row of the ridge table, which summarizes the number of trees remaining in field and LiDAR datasets when trees less than 18m tall were excluded. 14% (213) of trees remain in the field dataset compared to 36% (190) of trees remaining in the LiDAR dataset; at the 18m height cutoff, there were 23 more trees in the field dataset than the LiDAR dataset.

Table 3. a) DTK pairwise comparisons of basal area per hectare variables.

	BA/ha of Individual Trees		BA/ha of Small Clumps		BA/ha of Medium Clumps		BA/ha (All Trees Pooled)	
	Significant?	Difference	Significant?	Difference	Significant?	Difference	Significant?	Difference
Shallow Northerly - Canyon	N	0.2	N	0.0	N	0.0	N	0.0
Steep Northerly - Canyon	**Y**	**-2.3**	N	-0.4	N	0.2	N	-2.6
Ridge - Canyon	**Y**	**-3.9**	**Y**	**-2.2**	N	-0.4	**Y**	**-6.6**
Shallow Southerly - Canyon	N	-0.7	N	-0.4	N	-0.3	N	-1.7
Steep Southerly - Canyon	**Y**	**-4.6**	**Y**	**-3.1**	**Y**	**-0.7**	**Y**	**-8.7**
Steep Northerly - Shallow Northerly	**Y**	**-2.5**	N	-0.4	N	0.2	N	-2.7
Ridge - Shallow Northerly	**Y**	**-4.1**	**Y**	**-2.2**	N	-0.3	**Y**	**-6.6**
Shallow Southerly - Shallow Northerly	N	-0.9	N	-0.5	N	-0.3	N	-1.7
Steep Southerly - Shallow Northerly	**Y**	**-4.8**	**Y**	**-3.1**	**Y**	**-0.7**	**Y**	**-8.7**
Ridge - Steep Northerly	**Y**	**-1.6**	**Y**	**-1.8**	N	-0.5	**Y**	**-3.9**
Shallow Southerly - Steep Northerly	**Y**	**1.6**	N	0.0	N	-0.5	N	1.0
Steep Southerly - Steep Northerly	**Y**	**-2.3**	**Y**	**-2.7**	**Y**	**-0.8**	**Y**	**-6.0**
Shallow Southerly - Ridge	**Y**	**3.2**	**Y**	**1.8**	N	0.0	**Y**	**4.9**
Steep Southerly - Ridge	N	-0.7	N	-0.9	N	-0.3	N	-2.1
Steep Southerly - Shallow Southerly	**Y**	**-3.9**	**Y**	**-2.7**	**Y**	**-0.4**	**Y**	**-7.0**

Table 3. b) DTK pairwise comparisons of basal area per clump variables.

	Avg. BA of Indivduals		Avg. BA of Small Clumps		Avg. BA of Medium Clumps	
	Significant?	Difference	Significant?	Difference	Significant?	Difference
Shallow Northerly - Canyon	N	0.01	N	0.05	N	0.00
Steep Northerly - Canyon	**Y**	**-0.05**	N	-0.07	N	-0.29
Ridge - Canyon	**Y**	**-0.08**	**Y**	**-0.14**	**Y**	**-0.37**
Shallow Southerly - Canyon	N	0.00	N	0.04	N	-0.07
Steep Southerly - Canyon	**Y**	**-0.08**	**Y**	**-0.13**	N	-0.36
Steep Northerly - Shallow Northerly	**Y**	**-0.06**	**Y**	**-0.12**	N	-0.29
Ridge - Shallow Northerly	**Y**	**-0.09**	**Y**	**-0.19**	**Y**	**-0.37**
Shallow Southerly - Shallow Northerly	N	-0.01	N	-0.01	N	-0.07
Steep Southerly - Shallow Northerly	**Y**	**-0.09**	**Y**	**-0.18**	**Y**	**-0.37**
Ridge - Steep Northerly	N	-0.03	N	-0.07	N	-0.09
Shallow Southerly - Steep Northerly	**Y**	**0.05**	N	0.11	N	0.22
Steep Southerly - Steep Northerly	N	-0.02	N	-0.07	N	-0.08
Shallow Southerly - Ridge	**Y**	**0.08**	**Y**	**0.18**	**Y**	**0.30**
Steep Southerly - Ridge	N	0.01	N	0.01	N	0.01
Steep Southerly - Shallow Southerly	**Y**	**-0.07**	**Y**	**-0.17**	N	-0.30

Table 3 – continued. c) DTK pairwise comparisons of tree density variables.

	# Individual Trees/ha		# Trees in Small Clumps/ha		# Trees in Medium Clumps/ha		# Trees/ha (All Trees Pooled)	
	Significant?	Difference	Significant?	Difference	Significant?	Difference	Significant?	Difference
Shallow Northerly - Canyon	N	-0.5	N	-1.9	N	-0.5	N	-3.5
Steep Northerly - Canyon	N	-2.8	N	1.3	N	1.0	N	-1.0
Ridge - Canyon	**Y**	**-7.0**	N	-4.4	N	-1.0	N	-12.9
Shallow Southerly - Canyon	N	-2.0	N	-2.9	N	-1.4	N	-7.1
Steep Southerly - Canyon	**Y**	**-10.4**	**Y**	**-8.5**	N	-2.3	**Y**	**-22.3**
Steep Northerly - Shallow Northerly	N	-2.3	N	3.3	N	1.5	N	2.4
Ridge - Shallow Northerly	**Y**	**-6.5**	N	-2.5	N	-0.5	N	-9.5
Shallow Southerly - Shallow Northerly	N	-1.5	N	-1.0	N	-0.8	N	-3.6
Steep Southerly - Shallow Northerly	**Y**	**-10.0**	**Y**	**-6.6**	N	-1.8	**Y**	**-18.9**
Ridge - Steep Northerly	N	-4.2	**Y**	**-5.8**	N	-2.0	**Y**	**-11.9**
Shallow Southerly - Steep Northerly	N	0.8	**Y**	**-4.2**	**Y**	**-2.4**	N	-6.1
Steep Southerly - Steep Northerly	**Y**	**-7.6**	**Y**	**-9.8**	**Y**	**-3.3**	**Y**	**-21.3**
Shallow Southerly - Ridge	**Y**	**5.0**	N	1.5	N	-0.4	N	5.8
Steep Southerly - Ridge	N	-3.4	N	-4.1	N	-1.3	N	-9.4
Steep Southerly - Shallow Southerly	**Y**	**-8.4**	**Y**	**-5.6**	N	-1.0	**Y**	**-15.2**

Table 3d. DTK pairwise comparisons of average diameter variables.

	Avg. DBH (cm) of Individuals		Avg. DBH(cm) of Trees in Small Clumps		Avg. DBH (cm) of Trees in Medium Clumps		Avg. DBH (cm) of All Trees Pooled	
	Significant?	Difference	Significant?	Difference	Significant?	Difference	Significant?	Difference
Shallow Northerly - Canyon	N	1.1	N	2.2	N	0.4	N	1.6
Steep Northerly - Canyon	**Y**	**-5.3**	N	-3.7	N	-4.6	N	-4.5
Ridge - Canyon	**Y**	**-8.2**	**Y**	**-5.9**	N	-5.6	**Y**	**-6.9**
Shallow Southerly - Canyon	N	-0.2	N	1.8	N	-0.3	N	0.8
Steep Southerly - Canyon	**Y**	**-7.3**	**Y**	**-5.3**	N	-4.5	**Y**	**-6.1**
Steep Northerly - Shallow Northerly	**Y**	**-6.4**	**Y**	**-5.9**	N	-5.0	**Y**	**-6.1**
Ridge - Shallow Northerly	**Y**	**-9.2**	**Y**	**-8.1**	**Y**	**-5.9**	**Y**	**-8.4**
Shallow Southerly - Shallow Northerly	N	-1.2	N	-0.4	N	-0.6	N	-0.7
Steep Southerly - Shallow Northerly	**Y**	**-8.4**	**Y**	**-7.5**	N	-4.9	**Y**	**-7.7**
Ridge - Steep Northerly	N	-2.8	N	-2.2	N	-0.9	N	-2.3
Shallow Southerly - Steep Northerly	**Y**	**5.2**	**Y**	**5.5**	N	4.4	**Y**	**5.3**
Steep Southerly - Steep Northerly	N	-1.9	N	-1.6	N	0.1	N	-1.6
Shallow Southerly - Ridge	**Y**	**8.0**	**Y**	**7.7**	N	5.3	**Y**	**7.7**
Steep Southerly - Ridge	N	0.9	N	0.6	N	1.0	N	0.8
Steep Southerly - Shallow Southerly	**Y**	**-7.1**	**Y**	**-7.1**	N	-4.2	**Y**	**-6.9**

Table 3e. DTK pairwise comparisons of average height variables.

	Avg. Ht. (m) of Individuals		Avg. Ht. (m) of Trees in Small Clumps		Avg. Ht. (m) of Trees in Medium Clumps		Av. Ht. (m) of All Trees Pooled	
	Significant?	Difference	Significant?	Difference	Significant?	Difference	Significant?	Difference
Shallow Northerly - Canyon	N	-0.4	N	0.1	N	-0.4	N	-0.1
Steep Northerly - Canyon	**Y**	**-2.4**	N	-1.7	**Y**	**-1.8**	**Y**	**-2.0**
Ridge - Canyon	**Y**	**-4.7**	**Y**	**-3.8**	**Y**	**-3.5**	**Y**	**-4.2**
Shallow Southerly - Canyon	N	-1.0	N	-0.2	N	-0.8	N	-0.6
Steep Southerly - Canyon	**Y**	**-3.6**	**Y**	**-2.8**	**Y**	**-2.4**	**Y**	**-3.1**
Steep Northerly - Shallow Northerly	**Y**	**-2.0**	**Y**	**-1.8**	N	-1.4	**Y**	**-1.9**
Ridge - Shallow Northerly	**Y**	**-4.3**	**Y**	**-4.0**	**Y**	**-3.1**	**Y**	**-4.1**
Shallow Southerly - Shallow Northerly	N	-0.6	N	-0.3	N	-0.3	N	-0.5
Steep Southerly - Shallow Northerly	**Y**	**-3.2**	**Y**	**-2.9**	**Y**	**-2.0**	**Y**	**-3.0**
Ridge - Steep Northerly	**Y**	**-2.3**	**Y**	**-2.2**	**Y**	**-1.7**	**Y**	**-2.2**
Shallow Southerly - Steep Northerly	N	1.4	N	1.4	N	1.0	N	1.4
Steep Southerly - Steep Northerly	N	-1.2	N	-1.1	N	-0.6	N	-1.1
Shallow Southerly - Ridge	**Y**	**3.7**	**Y**	**3.6**	**Y**	**2.8**	**Y**	**3.6**
Steep Southerly - Ridge	N	1.1	N	1.0	N	1.1	N	1.1
Steep Southerly - Shallow Southerly	**Y**	**-2.6**	**Y**	**-2.6**	N	-1.7	**Y**	**-2.5**

Table 3 – continued. f) DTK pairwise comparisons of clump density variables and average clump size.

	Number of Small Clumps/ha		Number of Medium Clumps/ha		Mean Clump Size (Average Number of	
	Significant?	Difference	Significant?	Difference	Significant?	Difference
Shallow Northerly - Canyon	N	-0.7	N	-0.1	N	-0.1
Steep Northerly - Canyon	N	0.4	N	0.2	N	-0.1
Ridge - Canyon	N	-1.8	N	-0.1	N	0.0
Shallow Southerly - Canyon	N	-1.1	N	-0.2	N	-0.4
Steep Southerly - Canyon	**Y**	**-3.5**	N	-0.4	N	-0.5
Steep Northerly - Shallow Northerly	N	1.1	N	0.3	N	0.0
Ridge - Shallow Northerly	N	-1.1	N	-0.1	N	0.1
Shallow Southerly - Shallow Northerly	N	-0.4	N	-0.1	N	-0.3
Steep Southerly - Shallow Northerly	**Y**	**-2.8**	N	-0.3	N	-0.4
Ridge - Steep Northerly	**Y**	**-2.2**	N	-0.3	N	0.0
Shallow Southerly - Steep Northerly	N	-1.5	**Y**	**-0.4**	N	-0.3
Steep Southerly - Steep Northerly	**Y**	**-3.9**	**Y**	**-0.6**	**Y**	**-0.4**
Shallow Southerly - Ridge	N	0.7	N	-0.1	N	-0.3
Steep Southerly - Ridge	N	-1.7	N	-0.2	N	-0.5
Steep Southerly - Shallow Southerly	**Y**	**-2.4**	N	-0.2	N	-0.1

Table 3. Dunnett's-modified Tukey-Kramer's pairwise comparison results. In these tests, each of the six landforms were compared to one another for a total of 15 pairwise comparisons. Variable estimates from landforms on the right side of the "-" symbol were subtracted from landform estimates on the left side; a negative difference means the variable estimate was higher on the landform after the "–" symbol than the one before. Significant differences are indicated by a bolded "Y" in the "Significance?" column and estimated differences are provided in the "Difference" column (significant differences are also bolded); these difference values are the centers of 95% confidence intervals. If 95% confidence intervals contained 0, differences in variables estimates were deemed non-significant (non-bolded table entries). The table is split into sub-tables of six variable groups: a) basal area per hectare variables; b) basal area per clump variables; c) tree density variables; d) average diameter variables; e) average height variables; f) clump density variables and mean clump size. There were no significant differences between any pairs of landforms for large clump variables and these were not included in any sub-tables.

Figures

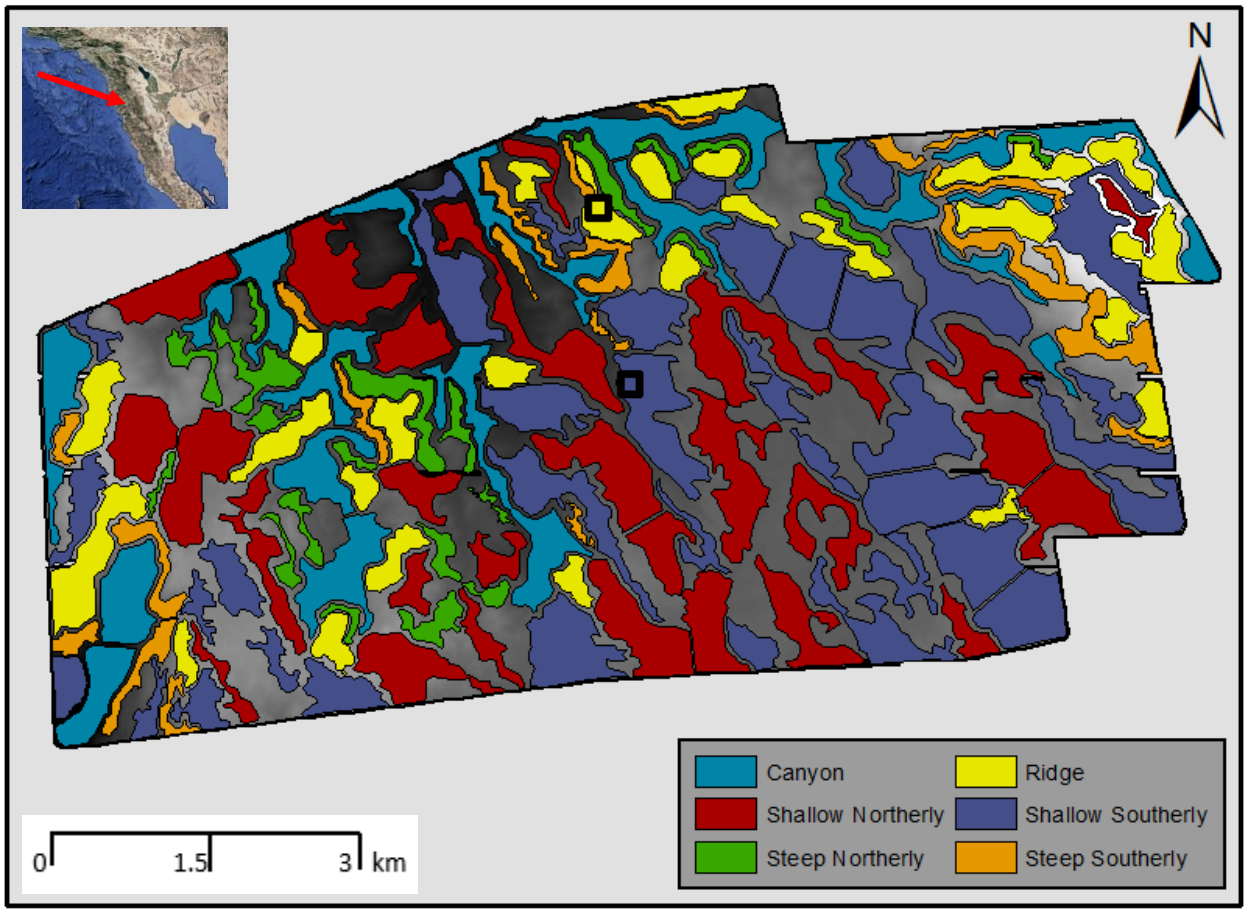

Figure 1. Location of the study area in Mexico (upper-left inset) and the SSPM LiDAR acquisition area (~6,500 hectares). Colored polygons represent landforms: canyon = blue; shallow northerly slopes = red; steep northerly slopes = green; ridge = yellow; shallow southerly slopes = purple; and steep southerly slopes = orange. Shallow refers to slopes ‹ 30% in grade; steep refers to slopes › 30%; northerly refers to aspects from 316 – 135°; and southerly refers to aspects from 136 – 315°. The two hollow black squares indicate the location of the Fry plots; the northernmost square bounds the ridge plot, and the southernmost square bounds the shallow southerly (SHS) plot.

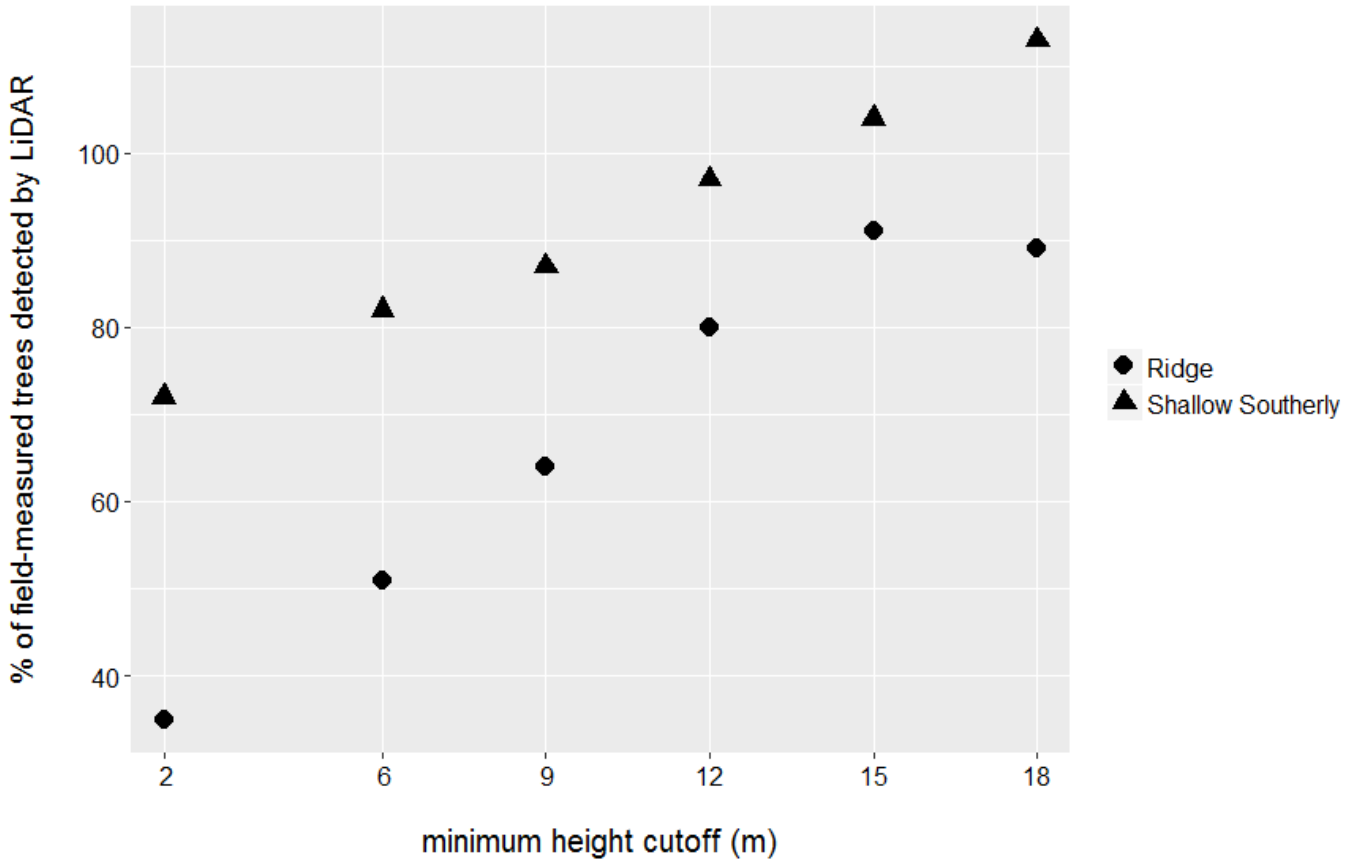

Figure 2. Effect of minimum height cutoff (x-axis) on the percent of field-measured trees detected from LiDAR by TreeSeg on the high-density ridge (blue) and low-density shallow southerly (orange) plot. Above the 12m cutoff, LiDAR overestimated actual tree numbers on the shallow southerly plot, and agreement in tree number between data sources on the ridge plot was maximized at the 15m cutoff.

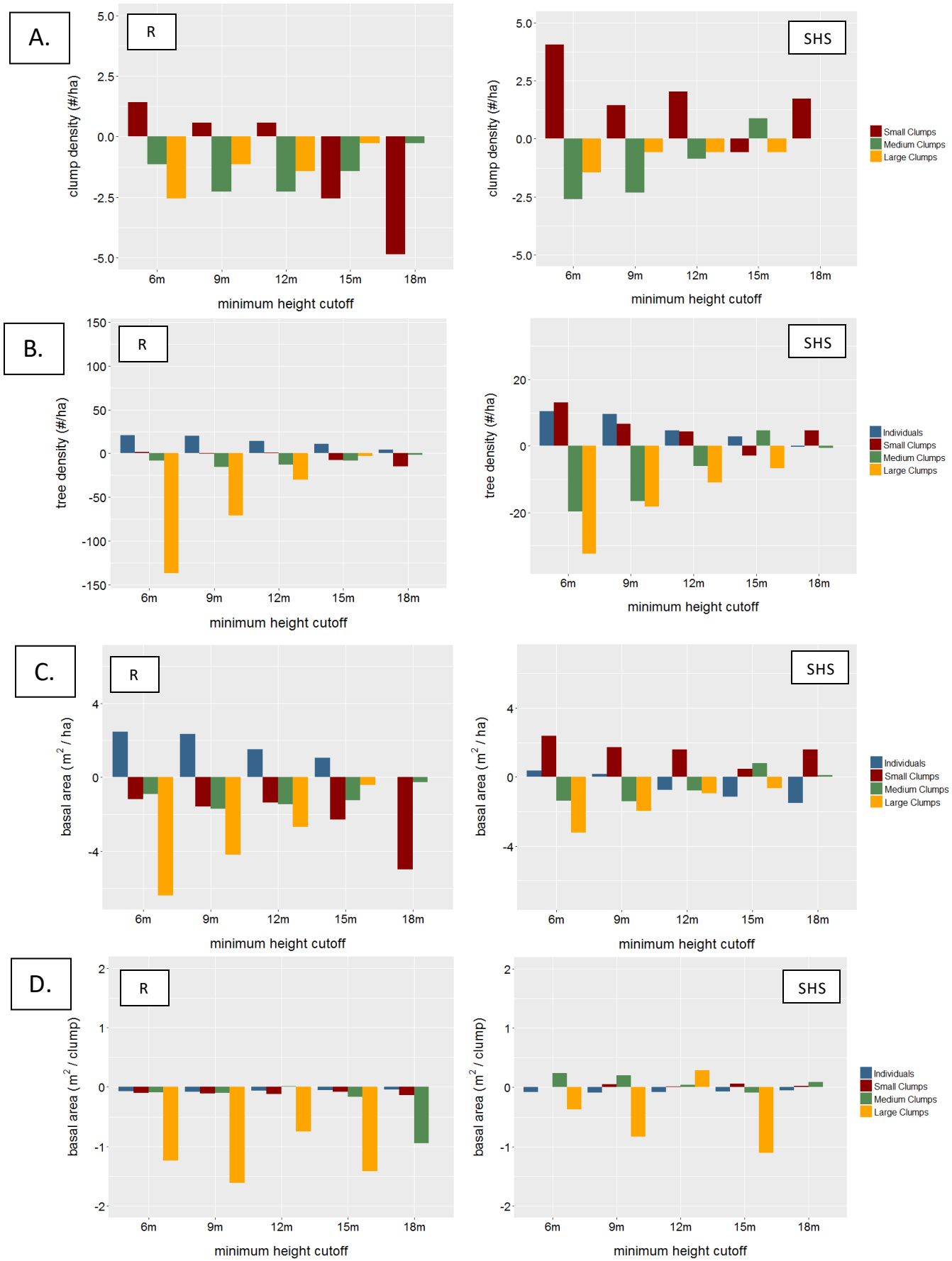

Figure 3. Difference between field and LiDAR estimates of: number of small clumps (2-4 trees, red), medium clumps (5-9 trees, green), and large clumps (>10 trees, yellow) per hectare (panel A); number of trees per hectare as individuals (blue) or in small, medium and large clumps (panel B); basal area per hectare of all clump size classes (panel C); and basal area of each clump size class (panel D). The ridge plot (R) is shown on the left and the shallow southerly (SHS) plot on the right. Negative bars indicate that the LiDAR estimate was lower than the field estimate.

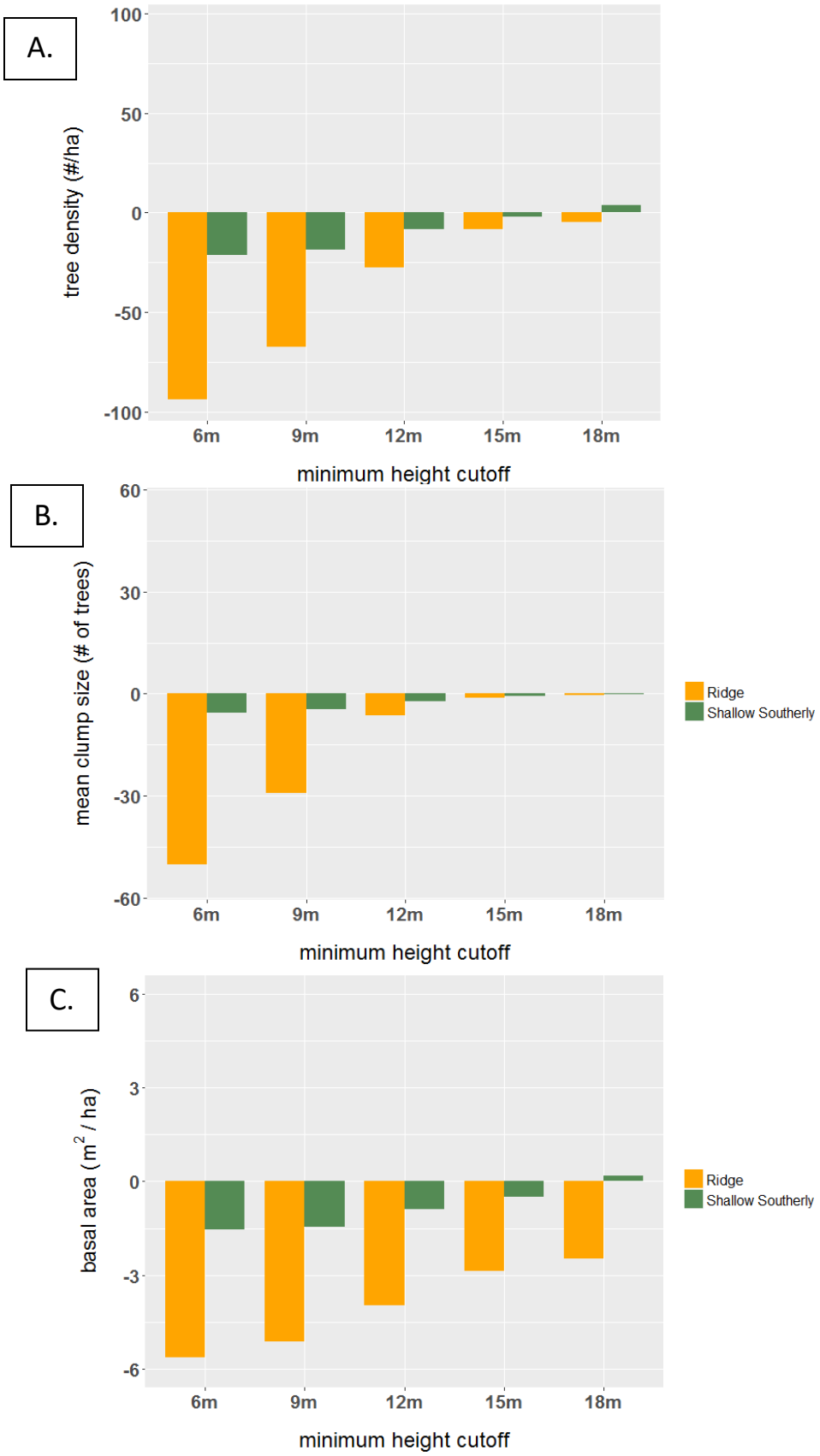

Figure 4. Difference between field and LiDAR estimates of the number of trees per hectare for all trees pooled (panel A); mean clump size (average number of trees in clumps) (panel B); and basal area per hectare of all trees pooled (panel C). Negative bars indicate that the LiDAR estimate was lower than the field estimate.

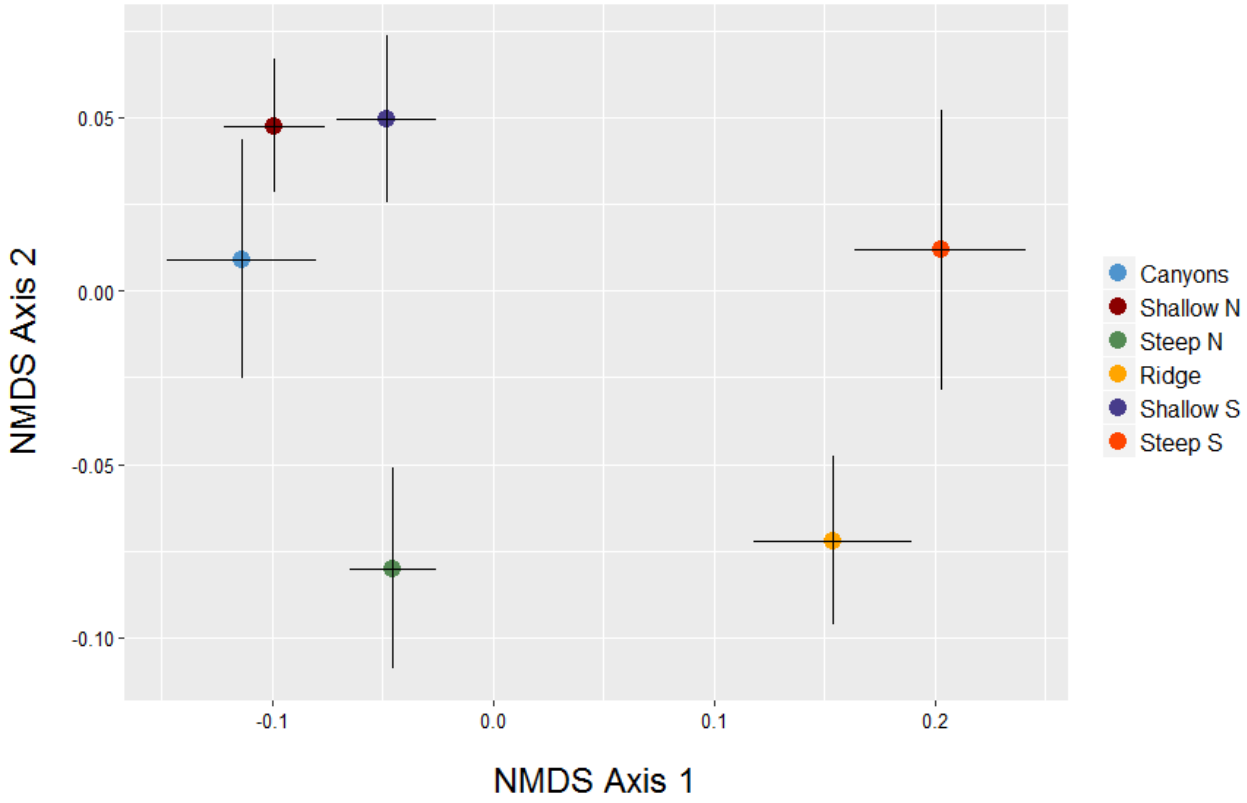

Figure 5. NMDS ordination considering the relationship among six landforms (canyon = blue, shallow northerly = red, steep northerly = green, ridge = yellow, shallow southerly = purple, and steep southerly = orange) in ordination space based on 25 stand-level and spatial pattern structure variables. NMDS Axis 1 accounts for primary sources of variation (a combination of variables) among landforms, and Axis 2 represents secondary sources of variation among landforms. Horizontal lines represent standard error of NMDS Axis 1 scores and vertical lines represent standard error of NMDS Axis 2 scores.

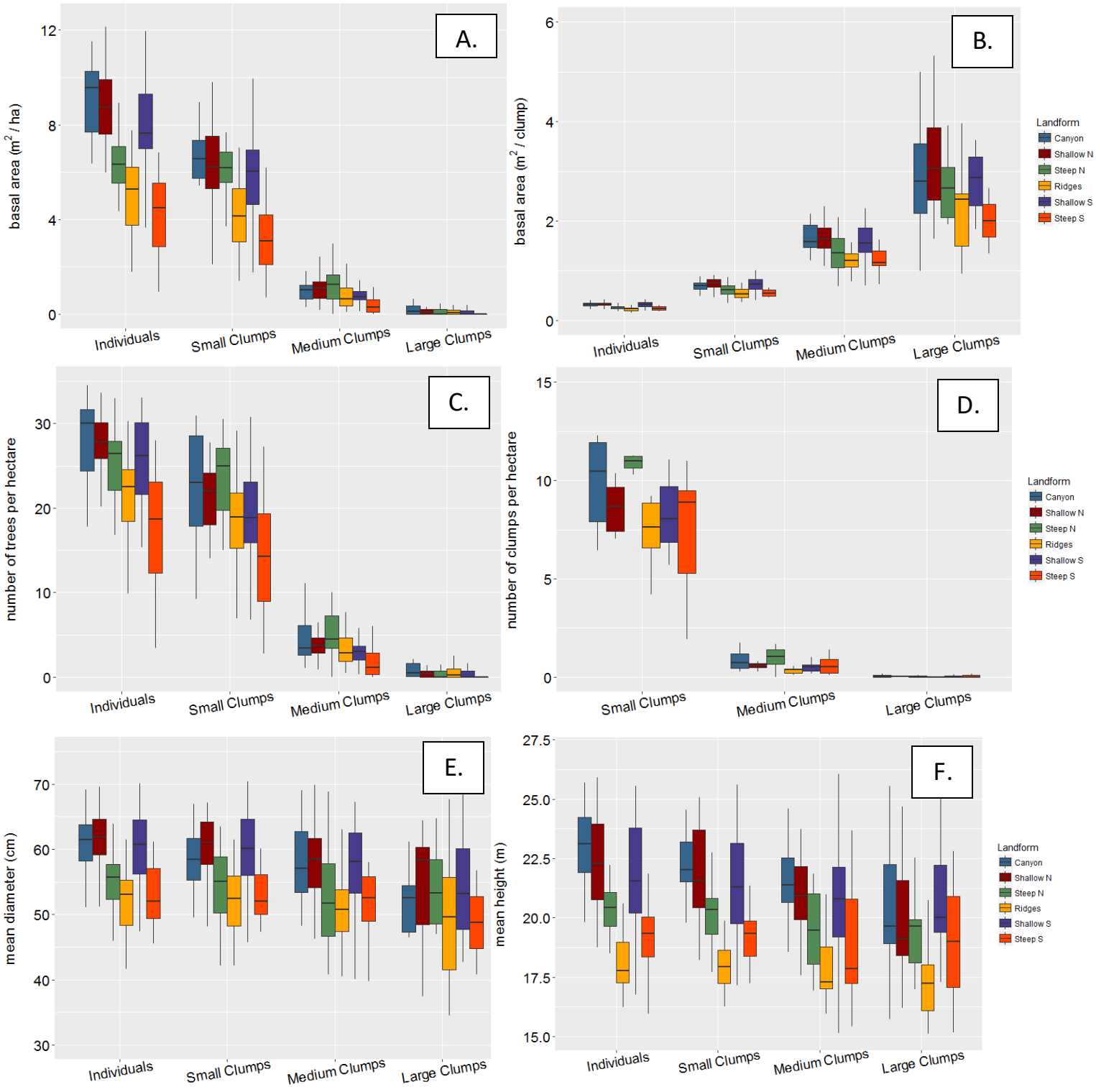

Figure 6. Boxplots of spatial pattern variables for six landforms by clump size class (individual trees lack close neighbors, small clumps have 2-4 trees, medium clumps have 5-9 trees, and large clumps have 10 or more trees). Canyons (blue), shallow northerly slopes (red), and shallow southerly slopes (purple) tend to have more, taller trees than ridges (yellow) and steep southerly slopes (orange) across clump sizes; spatial pattern on steep northerly slopes (green) is often similar to canyons and shallow slopes but can also be similar to ridges and steep southerly slopes. A) basal area per hectare (m^2); B) basal area per clump (m^2); C) number of trees per hectare; D) number of clumps per hectare (does not include individuals); E) average diameter (cm); and F) average height (m).

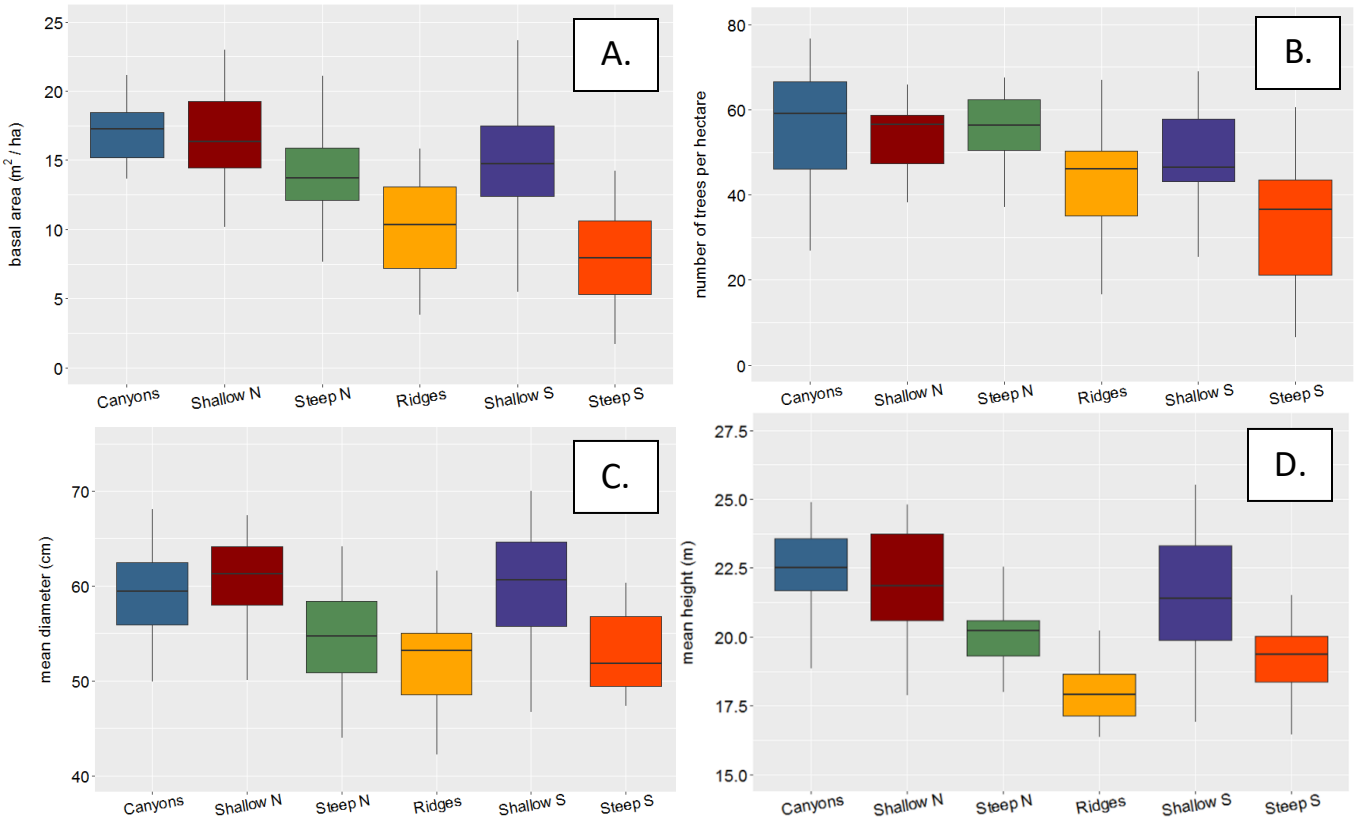

Figure 7. Boxplots of stand-level structure variables (all trees pooled, regardless of membership in clumps) for six landforms. Canyons (blue), shallow northerly slopes (red), and shallow southerly slopes (purple) tend to have more, taller trees than ridges (yellow) and steep southerly slopes (orange); stand-level structure on steep northerly slopes (green) is often similar to canyons and shallow slopes but can also be similar to ridges and steep southerly slopes. A) basal area per hectare (m^2); B) number of trees per hectare; C) average diameter (cm); and D) average height (m).

Supplementary Appendix

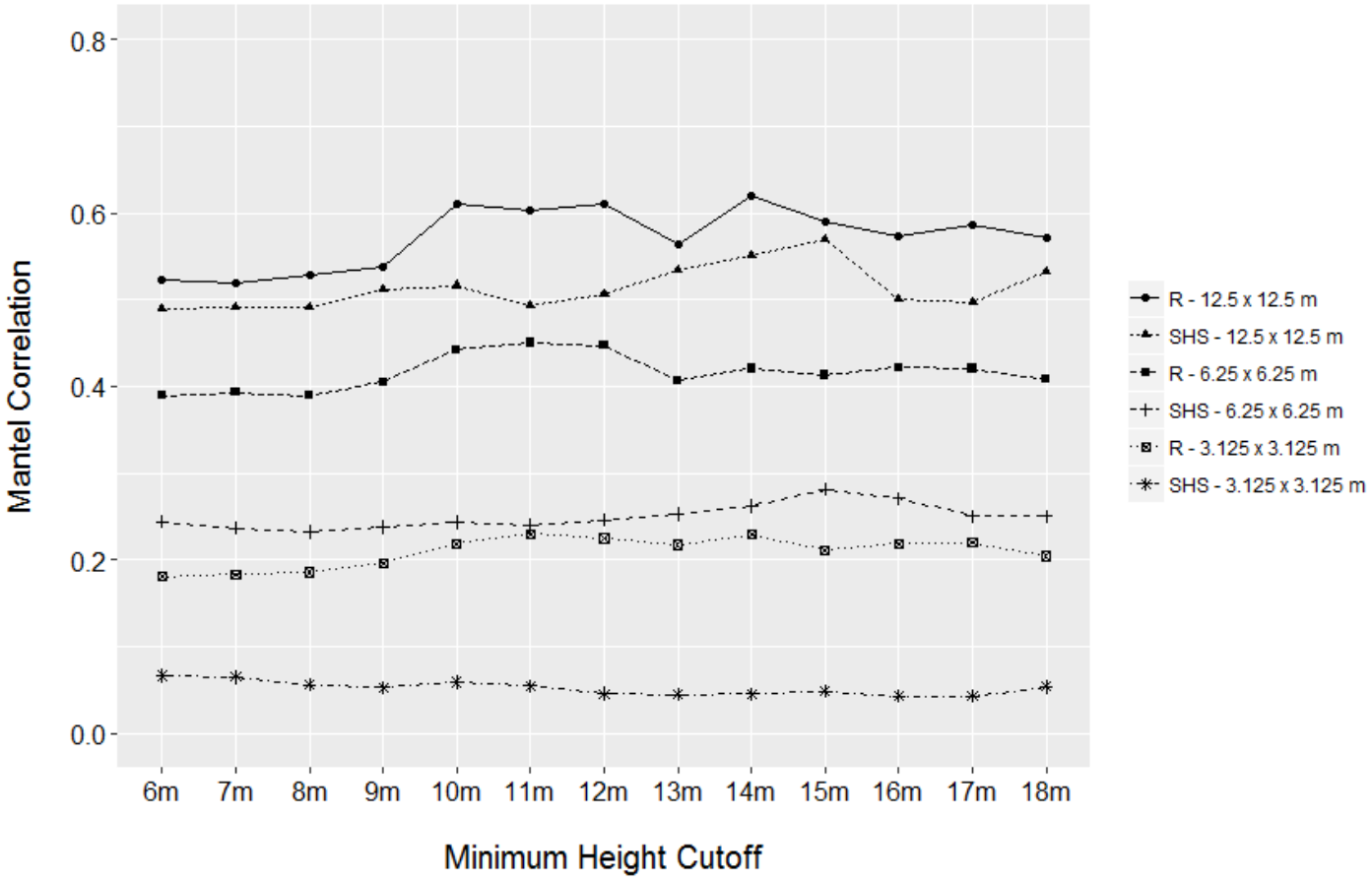

Figure 1. Correlation between LiDAR- and field-based spatial maps of tree density as a function of minimum tree height at three grain sizes: 3.125 by 3.125 m (9.77 m^2), 6.25 x 6.25 m (39.0625m^2), and 12.5 x 12.5m (156.25m^2) for the ridge (R) and shallow southerly (SHS) plots.

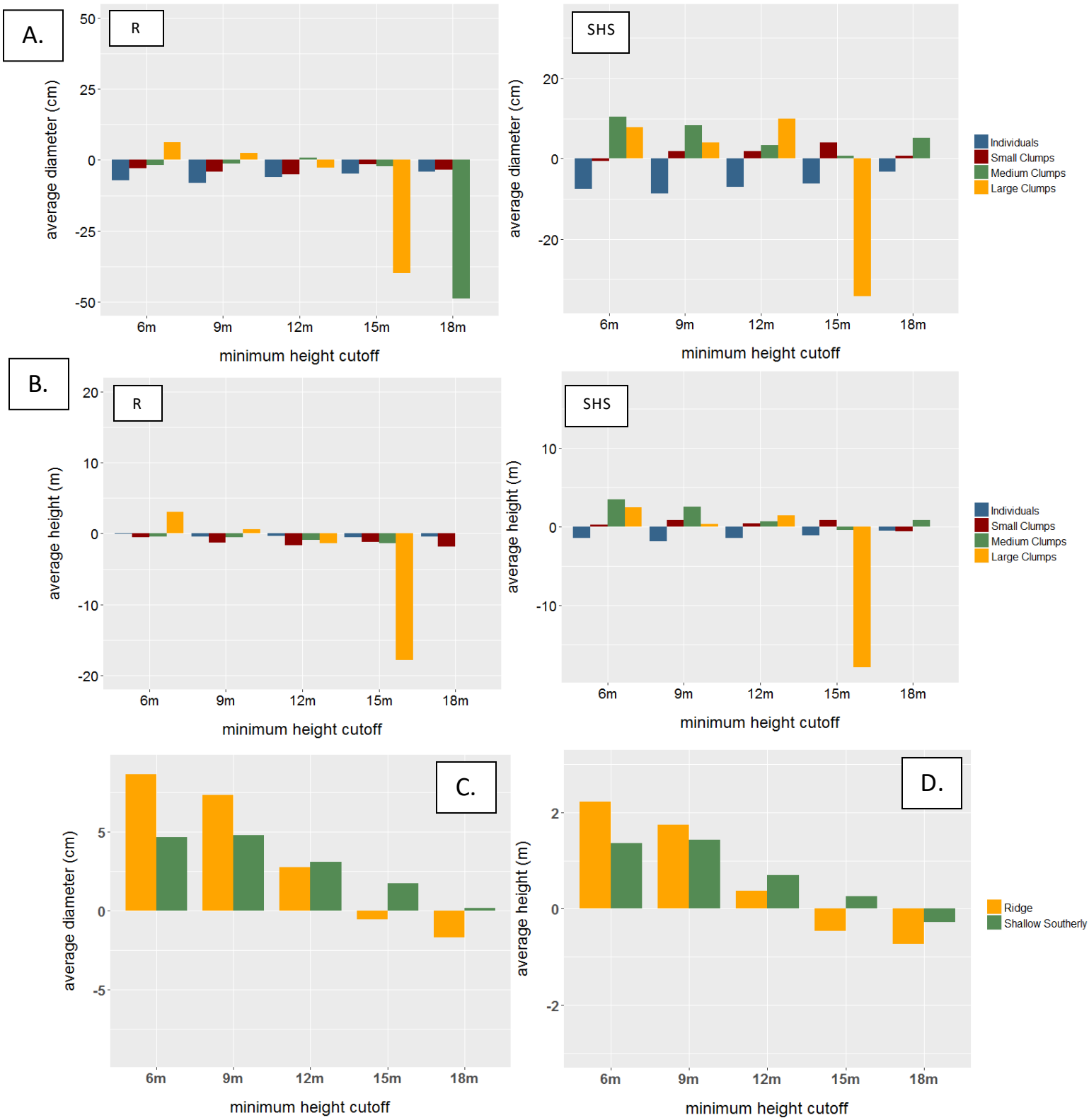

Figure 2. Difference in tree size estimates (average diameter and average height). Negative bars indicate that the LiDAR estimate was lower than the field estimate and positive bars indicate that the LiDAR estimate was greater than what was observed in the field. Panel A shows the difference in estimates of average diameter of individual trees (blue), small clumps (2-4 trees, red), medium clumps (5-9 trees, green), and large clumps (10+ trees, yellow); the ridge plot (R) is shown on the left and the shallow southerly plot (SHS) on the right. Panel B is the same except it shows the difference in estimates of average height. The difference in average diameter when all trees are pooled is shown on the left in panel C and the difference in average height for all trees pooled is shown on the right in panel D.

Canyons						
Individuals						
	BA/ha	BA/tree	# trees/ha	Av. Diam (cm)	Av. Height (m)	
Minimum	2.8	0.2	12.6	51.1	16.1	
25th percentile	7.7	0.3	24.4	58.2	21.9	
Median	9.5	0.3	30.0	61.5	23.1	
Mean	8.8	0.3	27.8	60.6	22.7	
75th percentile	10.2	0.3	31.7	63.8	24.2	
Maximum	11.5	0.4	34.5	69.2	25.7	
Small Clumps						
	BA/ha	BA/tree	# trees/ha	# clumps/ha	Av. Diam (cm)	Av. Height (m)
Minimum	2.9	0.5	9.2	4.2	49.5	16.0
25th percentile	5.7	0.6	17.9	7.6	55.2	21.5
Median	6.6	0.7	23.0	9.7	58.4	22.0
Mean	6.4	0.7	22.7	9.4	58.2	21.8
75th percentile	7.3	0.8	28.6	11.7	61.7	23.2
Maximum	8.9	0.9	30.9	12.5	67.0	24.6
Medium Clumps						
	BA/ha	BA/tree	# trees/ha	# clumps/ha	Av. Diam (cm)	Av. Height (m)
Minimum	0.3	1.2	1.0	0.2	48.3	17.1
25th percentile	0.6	1.5	2.6	0.4	53.4	20.7
Median	1.0	1.6	3.4	0.6	57.1	21.4
Mean	1.1	1.6	4.3	0.7	57.4	21.4
75th percentile	1.2	1.9	6.1	1.0	62.8	22.5
Maximum	2.7	2.1	11.1	1.8	69.0	24.6
Large Clumps						
	BA/ha	BA/tree	# trees/ha	# clumps/ha	Av. Diam (cm)	Av. Height (m)
Minimum	0.0	1.0	0.0	0.0	34.8	15.7
25th percentile	0.0	2.2	0.1	0.0	47.5	18.9
Median	0.1	2.8	0.5	0.0	52.8	19.6
Mean	0.3	2.8	1.2	0.1	52.3	20.1
75th percentile	0.3	3.6	1.6	0.1	57.2	22.3
Maximum	1.9	5.0	9.0	0.4	77.1	25.6
All Trees Pooled						
	BA/ha	# trees/ha	Av. Diam. (cm)	Av. Height (m)	MCS (av. # trees/clump)	
Minimum	5.9	26.9	49.9	16.2	1.6	
25th percentile	15.2	46.0	55.9	21.7	1.9	
Median	17.2	59.1	59.5	22.5	2.1	
Mean	16.5	56.0	59.2	22.2	2.4	
75th percentile	18.5	66.6	62.5	23.6	2.3	
Maximum	21.1	76.6	68.1	24.9	7.1	

Shallow Northerly						
Individuals						
	BA/ha	BA/tree	# trees/ha	Av. Diam (cm)	Av. Height (m)	
Minimum	4.1	0.2	13.2	51.2	18.8	
25th percentile	7.7	0.3	25.9	59.1	20.8	
Median	8.8	0.3	27.8	61.9	22.3	
Mean	8.9	0.3	27.4	61.7	22.4	
75th percentile	10.2	0.4	30.2	64.6	24.0	
Maximum	12.6	0.4	33.6	69.6	25.9	
Small Clumps						
	BA/ha	BA/tree	# trees/ha	# clumps/ha	Av. Diam (cm)	Av. Height (m)
Minimum	2.1	0.5	6.3	2.7	48.2	18.2
25th percentile	5.3	0.7	18.0	7.5	57.7	20.4
Median	6.2	0.8	22.0	9.1	61.0	21.6
Mean	6.4	0.7	20.7	8.7	60.4	21.9
75th percentile	7.5	0.8	24.2	10.2	64.2	23.7
Maximum	9.8	0.9	27.7	11.7	67.1	25.1
Medium Clumps						
	BA/ha	BA/tree	# trees/ha	# clumps/ha	Av. Diam (cm)	Av. Height (m)
Minimum	0.2	1.1	0.9	0.2	46.3	17.6
25th percentile	0.7	1.5	2.8	0.5	54.1	19.9
Median	1.1	1.6	3.7	0.7	58.4	20.9
Mean	1.1	1.6	3.8	0.6	57.8	21.0
75th percentile	1.4	1.9	4.6	0.8	61.7	22.2
Maximum	2.4	2.3	10.0	1.6	69.9	23.7
Large Clumps						
	BA/ha	BA/tree	# trees/ha	# clumps/ha	Av. Diam (cm)	Av. Height (m)
Minimum	0.0	1.6	0.0	0.0	37.5	13.4
25th percentile	0.0	2.4	0.0	0.0	48.7	18.4
Median	0.1	3.1	0.4	0.0	59.5	19.1
Mean	0.1	3.4	0.7	0.0	55.2	20.1
75th percentile	0.2	4.0	0.7	0.1	60.5	22.1
Maximum	0.7	7.4	5.9	0.2	77.9	28.6
All Trees Pooled						
	BA/ha	# trees/ha	Av. Diam. (cm)	Av. Height (m)	MCS (av. # trees/clump)	
Minimum	6.5	20.9	50.0	17.9	1.6	
25th percentile	14.4	47.4	58.0	20.6	1.9	
Median	16.3	56.5	61.3	21.9	2.0	
Mean	16.6	52.6	60.7	22.0	2.3	
75th percentile	19.3	58.6	64.1	23.8	2.2	
Maximum	23.0	65.8	67.5	24.8	8.1	

Steep Northerly						
Individuals						
	BA/ha	BA/tree	# trees/ha	Av. Diam (cm)	Av. Height (m)	
Minimum	4.3	0.2	16.8	45.9	18.5	
25th percentile	5.5	0.2	22.1	52.4	19.7	
Median	6.3	0.3	26.5	55.7	20.4	
Mean	6.5	0.3	25.0	55.2	20.4	
75th percentile	7.1	0.3	27.9	57.7	21.1	
Maximum	8.9	0.3	33.0	63.9	22.2	
Small Clumps						
	BA/ha	BA/tree	# trees/ha	# clumps/ha	Av. Diam (cm)	Av. Height (m)
Minimum	3.3	0.4	15.0	6.7	42.1	17.7
25th percentile	5.6	0.5	19.8	8.1	50.3	19.3
Median	6.2	0.6	25.0	10.3	55.1	20.3
Mean	6.0	0.6	24.0	9.9	54.5	20.1
75th percentile	6.9	0.7	27.1	11.0	58.8	20.8
Maximum	9.0	0.9	30.5	12.5	63.4	22.8
Medium Clumps						
	BA/ha	BA/tree	# trees/ha	# clumps/ha	Av. Diam (cm)	Av. Height (m)
Minimum	0.0	0.7	0.0	0.0	40.8	16.9
25th percentile	0.6	1.1	3.4	0.6	46.7	18.1
Median	1.3	1.4	4.5	0.8	51.7	19.5
Mean	1.3	1.3	5.3	0.9	52.8	19.6
75th percentile	1.7	1.7	7.2	1.2	57.8	21.0
Maximum	3.0	2.1	10.0	1.7	68.8	21.8
Large Clumps						
	BA/ha	BA/tree	# trees/ha	# clumps/ha	Av. Diam (cm)	Av. Height (m)
Minimum	0.0	1.9	0.0	0.0	47.0	17.0
25th percentile	0.0	2.1	0.0	0.0	48.6	18.1
Median	0.0	2.7	0.0	0.0	53.3	19.6
Mean	0.2	2.7	0.6	0.1	54.1	19.3
75th percentile	0.2	3.1	0.7	0.1	58.4	19.9
Maximum	1.2	3.9	4.6	0.4	64.7	22.5
All Trees Pooled						
	BA/ha	# trees/ha	Av. Diam. (cm)	Av. Height (m)	MCS (av. # trees/clump)	
Minimum	7.6	37.2	44.0	18.0	1.7	
25th percentile	12.1	50.5	50.8	19.3	2.0	
Median	13.7	56.3	54.7	20.2	2.3	
Mean	13.9	55.0	54.6	20.2	2.3	
75th percentile	15.9	62.4	58.4	20.6	2.5	
Maximum	21.1	67.5	64.2	22.5	3.3	

Ridge						
Individuals						
	BA/ha	BA/tree	# trees/ha	Av. Diam (cm)	Av. Height (m)	
Minimum	1.8	0.2	8.0	41.7	16.2	
25th percentile	3.7	0.2	18.5	48.4	17.3	
Median	5.3	0.2	22.5	53.1	17.8	
Mean	4.9	0.2	20.8	52.4	18.0	
75th percentile	6.2	0.3	24.5	55.3	19.0	
Maximum	7.8	0.3	30.3	61.5	20.6	
Small Clumps						
	BA/ha	BA/tree	# trees/ha	# clumps/ha	Av. Diam (cm)	Av. Height (m)
Minimum	1.4	0.4	5.4	2.2	42.1	16.3
25th percentile	3.1	0.5	15.3	6.5	48.2	17.2
Median	4.2	0.5	18.9	8.0	52.5	17.9
Mean	4.2	0.5	18.2	7.6	52.4	18.0
75th percentile	5.3	0.6	21.8	9.1	55.9	18.6
Maximum	7.0	0.8	29.1	11.5	61.5	19.9
Medium Clumps						
	BA/ha	BA/tree	# trees/ha	# clumps/ha	Av. Diam (cm)	Av. Height (m)
Minimum	0.1	0.8	0.5	0.1	40.5	15.9
25th percentile	0.3	1.1	1.9	0.3	47.4	17.0
Median	0.6	1.2	2.8	0.5	50.7	17.3
Mean	0.8	1.3	3.3	0.6	51.9	17.9
75th percentile	1.1	1.3	4.6	0.8	53.8	18.8
Maximum	2.1	2.1	9.2	1.5	70.0	22.2
Large Clumps						
	BA/ha	BA/tree	# trees/ha	# clumps/ha	Av. Diam (cm)	Av. Height (m)
Minimum	0.0	0.9	0.0	0.0	34.5	14.2
25th percentile	0.0	1.7	0.0	0.0	41.5	14.9
Median	0.1	2.4	0.3	0.0	49.7	16.3
Mean	0.1	2.6	0.7	0.1	49.3	16.7
75th percentile	0.2	2.5	1.0	0.1	55.7	17.3
Maximum	0.7	7.1	4.4	0.3	67.7	22.4
All Trees Pooled						
	BA/ha	# trees/ha	Av. Diam. (cm)	Av. Height (m)	MCS (av. # trees/clump)	
Minimum	3.8	16.6	42.2	16.4	1.7	
25th percentile	7.2	35.1	48.5	17.1	1.8	
Median	10.3	46.2	53.2	17.9	2.1	
Mean	9.9	43.1	52.3	18.0	2.3	
75th percentile	13.1	50.4	55.0	18.6	2.4	
Maximum	15.8	67.0	61.6	20.2	7.8	

Shallow Southerly						
Individuals						
	BA/ha	BA/tree	# trees/ha	Av. Diam (cm)	Av. Height (m)	
Minimum	3.7	0.2	15.3	47.4	16.8	
25th percentile	7.0	0.3	21.7	56.3	20.2	
Median	7.6	0.3	26.2	60.8	21.6	
Mean	8.1	0.3	25.8	60.4	21.7	
75th percentile	9.3	0.4	30.1	64.5	23.8	
Maximum	12.0	0.4	33.1	70.1	25.6	
Small Clumps						
	BA/ha	BA/tree	# trees/ha	# clumps/ha	Av. Diam (cm)	Av. Height (m)
Minimum	1.7	0.4	6.8	3.1	45.8	17.1
25th percentile	4.6	0.6	15.9	6.8	56.0	19.8
Median	6.0	0.7	18.8	8.1	60.2	21.3
Mean	5.9	0.7	19.8	8.3	60.1	21.6
75th percentile	6.9	0.8	23.1	9.7	64.6	23.1
Maximum	9.9	1.0	30.8	13.0	70.4	25.6
Medium Clumps						
	BA/ha	BA/tree	# trees/ha	# clumps/ha	Av. Diam (cm)	Av. Height (m)
Minimum	0.1	0.7	0.3	0.1	38.1	15.1
25th percentile	0.6	1.4	2.0	0.3	53.2	19.2
Median	0.7	1.6	3.0	0.5	58.1	20.8
Mean	0.8	1.6	3.0	0.5	57.1	20.6
75th percentile	0.9	1.9	3.6	0.6	62.6	22.1
Maximum	1.6	2.3	6.7	1.1	67.2	26.1
Large Clumps						
	BA/ha	BA/tree	# trees/ha	# clumps/ha	Av. Diam (cm)	Av. Height (m)
Minimum	0.0	1.8	0.0	0.0	42.7	14.6
25th percentile	0.0	2.3	0.0	0.0	47.8	19.3
Median	0.0	2.9	0.0	0.0	53.2	19.9
Mean	0.1	2.9	0.4	0.0	54.1	20.3
75th percentile	0.1	3.3	0.7	0.1	60.1	22.2
Maximum	0.5	5.6	2.5	0.2	68.6	25.8
All Trees Pooled						
	BA/ha	# trees/ha	Av. Diam. (cm)	Av. Height (m)	MCS (av. # trees/clump)	
Minimum	5.5	25.4	46.7	16.9	1.4	
25th percentile	12.4	43.1	55.8	19.9	1.8	
Median	14.8	46.4	60.6	21.4	2.0	
Mean	14.9	48.9	60.0	21.6	2.0	
75th percentile	17.5	57.8	64.6	23.3	2.1	
Maximum	23.7	69.0	70.0	25.5	3.5	

Steep Southerly						
Individuals						
	BA/ha	BA/tree	# trees/ha	Av. Diam (cm)	Av. Height (m)	
Minimum	0.9	0.2	3.4	45.5	15.9	
25th percentile	2.9	0.2	12.3	49.4	18.3	
Median	4.5	0.2	18.6	52.0	19.3	
Mean	4.1	0.2	17.4	53.3	19.1	
75th percentile	5.5	0.3	23.1	57.0	20.0	
Maximum	6.8	0.3	28.0	61.2	21.8	
Small Clumps						
	BA/ha	BA/tree	# trees/ha	# clumps/ha	Av. Diam (cm)	Av. Height (m)
Minimum	0.7	0.5	2.8	1.2	47.3	16.0
25th percentile	2.1	0.5	9.0	4.0	50.0	18.4
Median	3.1	0.5	14.3	6.2	52.0	19.3
Mean	3.3	0.6	14.2	6.0	52.9	19.0
75th percentile	4.2	0.6	19.3	8.4	56.1	19.9
Maximum	6.2	0.7	27.2	11.0	60.1	21.4
Medium Clumps						
	BA/ha	BA/tree	# trees/ha	# clumps/ha	Av. Diam (cm)	Av. Height (m)
Minimum	0.0	0.6	0.0	0.0	39.7	15.4
25th percentile	0.1	1.1	0.3	0.1	48.9	17.2
Median	0.3	1.2	1.1	0.2	52.6	17.9
Mean	0.4	1.3	2.0	0.4	52.9	19.0
75th percentile	0.6	1.4	2.9	0.5	55.8	20.8
Maximum	1.1	2.1	7.4	1.4	70.4	23.7
Large Clumps						
	BA/ha	BA/tree	# trees/ha	# clumps/ha	Av. Diam (cm)	Av. Height (m)
Minimum	0.0	1.3	0.0	0.0	40.8	15.2
25th percentile	0.0	1.7	0.0	0.0	44.8	17.1
Median	0.0	2.0	0.0	0.0	48.8	19.0
Mean	0.0	2.0	0.1	0.0	48.8	19.0
75th percentile	0.0	2.3	0.0	0.0	52.8	20.9
Maximum	0.4	2.7	1.5	0.2	56.8	22.8
All Trees Pooled						
	BA/ha	# trees/ha	Av. Diam. (cm)	Av. Height (m)	MCS (av. # trees/clump)	
Minimum	1.7	6.5	47.4	16.5	1.5	
25th percentile	5.3	21.2	49.4	18.4	1.6	
Median	7.9	36.6	51.8	19.4	1.8	
Mean	7.8	33.7	53.1	19.1	1.9	
75th percentile	10.6	43.5	56.8	20.0	2.1	
Maximum	14.2	60.6	60.3	21.5	2.5	